Cell Tissue Res (2014) 355:375–396
DOI 10.1007/s00441-013-1753-0

REGULAR ARTICLE

Angiostatin inhibits activation and migration of neutrophils

Gurpreet K. Aulakh · Yadu Balachandran · Lixin Liu · Baljit Singh

Received: 23 June 2013 / Accepted: 30 October 2013 / Published online: 3 December 2013
© Springer-Verlag Berlin Heidelberg 2013

Abstract There is a critical need to identify molecules that modulate the biology of neutrophils because activated neutrophils, though necessary for host defense, cause exuberant tissue damage through production of reactive oxygen species and increased lifespan. Angiostatin, an endogenous anti-angiogenic cleavage product of plasminogen, binds to integrin $\alpha_v\beta_3$, ATP synthase and angiomotin and its expression is increased in inflammatory conditions. We test the hypothesis that angiostatin inhibits neutrophil activation, induces apoptosis and blocks recruitment in vivo and in vitro. The data show immuno-reactivity for plasminogen/angiostatin in resting neutrophils. Angiostatin conjugated to FITC revealed that angiostatin was endocytozed by activated mouse and human neutrophils in a lipid raft-dependent fashion. Co-immunoprecipitation of human neutrophil lysates, confocal microscopy of isolated mouse and human neutrophils and functional blocking experiments showed that angiostatin complexes with flotillin-1 along with integrin $\alpha_v\beta_3$ and ATP synthase. Angiostatin inhibited fMLP-induced neutrophil polarization, as well as caused inhibition of hsp-27 phosphorylation and stabilization of microtubules. Angiostatin treatment, before or after LPS-induced neutrophil activation, inhibited phosphorylation of p38 and p44/42 MAPKs, abolished reactive oxygen species production and released the neutrophils from suppressed apoptosis, as indicated by expression of activated caspase-3 and morphological evidence of apoptosis. Finally, intravital microscopy and myeloperoxidase assay showed inhibition of neutrophil recruitment in post-capillary venules of TNFα-treated cremaster muscle in mouse. These in vitro and in vivo data demonstrate angiostatin as a broad deactivator and silencer of neutrophils and an inhibitor of their migration. These data potentially open new avenues for the development of anti-inflammatory drugs.

Keywords Neutrophil polarization · Apoptosis · Lipid raft · Integrin $\alpha_v\beta_3$ · Intravital microscopy

Introduction

The activation and migration of neutrophils are intricately linked at the molecular and cellular levels. There is a critical need to identify molecules that can effectively modulate both the migration and activation, because many acute inflammatory conditions such as peritonitis, pneumonia, sepsis, or sterile injury are marked by chemotaxis of activated neutrophils, an essential early step in innate host defense, towards the site of injury (Amulic et al. 2012). Activated neutrophils combat infections, while diverging from their constitutive programmed death to live longer. Persistent activation of neutrophils leads to secondary necrosis that, in turn, triggers production of reactive oxygen and nitrogen species that serve as signalling molecules and modulate neutrophil functions (Fialkow et al. 2007), further augmenting neutrophil recruitment and activation. This eventually is held responsible for collateral tissue damage and multiple complications in the injured organs (Witko-Sarsat 2010; Witko-Sarsat et al. 2000). Therefore, one of the critical needs is to identify novel molecules that regulate neutrophil migration and silence activated neutrophils, to prevent exuberant tissue damage.

Electronic supplementary material The online version of this article (doi:10.1007/s00441-013-1753-0) contains supplementary material, which is available to authorized users.

G. K. Aulakh · Y. Balachandran · B. Singh
Veterinary Biomedical Sciences, Western College of Veterinary Medicine, University of Saskatchewan, 52 Campus Drive, Saskatoon, SK S7N 5B4, Canada

L. Liu
Department of Pharmacology, College of Medicine, University of Saskatchewan, Saskatoon, Canada
e-mail: baljit.singh@usask.ca

Migration of activated neutrophils into inflamed organs occurs through development of one of the random pseudopods towards directional cues emanating from chemoattractants (Insall 2010; Insall and Machesky 2009). The key molecular events guiding the migration of neutrophils include aggregation of filamentous (F) actin to support extension of a major pseudopod also known as the leading edge. Chemoattractants bind to G-protein coupled receptors that signal through $\beta\gamma$ subunits via GTP-bound small G-proteins such as Rho, Rac and cdc42. Mitogen-activated protein kinases (MAPK) and phosphatases are activated downstream of the Rho family of GTP-binding small G proteins (Niggli 2003). Moreover, LPS stimulates neutrophils through p38 MAPK activation (Khan et al. 2005). During these events, the microtubule complex destabilizes through heat shock protein (hsp)-27 phosphorylation to favour formation of a major protrusion in vitro and a pseudopod in vivo (Hino and Hosoya 2003; Hino et al. 2000; Jog et al. 2007; Yoo et al. 2012). The trailing edge is often referred to as the uropod. The intracellular cytoskeletal elements are intricately linked to adhesive proteins such as integrins and selectins expressed on the surface of neutrophils (Barreiro et al. 2007, 2010; Ley et al. 2007). Neutrophils express and recycle the $\alpha_v\beta_3$ integrin during their directional movement in a Ca^{2+}-dependent manner and recently this integrin has been implicated in recruitment of neutrophils in endotoxin-induced lung inflammation (Lawson and Maxfield 1995; Moon et al. 2009; Rainger et al. 1999; Singh et al. 2005). Therefore, neutrophil migration occurs through highly coordinated molecular processes and cytoskeletal rearrangements.

Angiostatin is an endogenous protein generated after serial enzymatic proteolysis of plasminogen. Tumor cells, macrophages, platelets and neutrophils generate high amounts of angiostatin (Jurasz et al. 2006; O'Mahony et al. 1998; Scapini et al. 2002; Westphal et al. 2000). Angiostatin induces anoikis and apoptosis and inhibits endothelial and epithelial cell migration by binding to several cell surface proteins (Tabruyn and Griffioen 2007; Wahl et al. 2005) such as F_1F_0 ATP synthase (Kenan and Wahl 2005; Lee et al. 2009), hsp-27 (Dudani et al. 2007), annexin II (Sharma et al. 2006; Syed et al. 2007), $\alpha_v\beta_3$ integrin (Tarui et al. 2001) and angiomotin (Troyanovsky et al. 2001). We have learned about novel mechanisms of angiogenesis through the study of angiostatin biology and identification of its cellular target proteins (Kenan and Wahl 2005; Lee et al. 2009). Interestingly, angiostatin is also expressed in high amounts in bronchoalveolar lavage of patients with acute respiratory distress syndrome (ARDS) (Hamacher et al. 2002; Lucas et al. 2002) and has been shown to localize on the endothelium of lungs from sepsis patients through immunohistochemistry (Singh et al. 2005). Angiostatin inhibits monocyte as well as neutrophil chemotaxis in response to MCP-1, fMLP, IL-8, MIP-2, TPA and Gro-α in vitro (Benelli et al. 2002) and peripheral blood leukocyte recruitment and angiogenesis in a mouse model of acute peritonitis, whereby it inhibits tumor necrosis factor-α induced NFκB and tissue factor up-regulation (Chavakis et al. 2005). Both angiostatin *kringle* 1–4 and *kringle* 1–3 fragments show inhibitory activities in Boyden chambers, whereas plasminogen does not (Benelli et al. 2002). In contrast to this, plasminogen *kringle* 5 induces recruitment of tumor-associated neutrophils (Perri et al. 2007b). The actions of angiostatin are mediated through binding to integrin β_3, which is also expressed on neutrophils and plays a role in their migration (Lawson and Maxfield 1995; Rainger et al. 1999; Singh et al. 2000). However, other integrins such as β_1 and β_2 have also been shown to mediate angiostatin effects. Angiostatin K1-3 disrupts monocyte/macrophage actin cytoskeleton (Perri et al. 2007a). Moreover, neutrophils express most of the angiostatin-binding proteins such as F_1F_0 ATP synthase. Because neutrophils influence pathophysiology across multiple organs, there is a need to find fundamental ways to modulate their behaviour. As angiostatin K1-4 is more potent than the angiostatin K1-3 in inhibiting neutrophil chemotaxis in vitro (Benelli et al. 2002), we proposed and tested a hypothesis that angiostatin (K1-4) modulates neutrophil activation and directed migration.

Materials and methods

Reagents

Lipopolysaccharide from *E. coli* 0127:B8, LPS (L4516), fMLP, cytochalasin D (C2618), FluoroTag FITC Conjugation Kit (FITC1), 3,3′,5,5′-tetramethylbenzidine (TMB), cetyltrimethylammonium chloride, water-soluble cholesterol (C4951) and methyl-β-cyclodextrin (C4555) were obtained from Sigma Chemicals (St. Louis, MO, USA); purified angiostatin K1-4 was commercially obtained from Haematologic Technologies Inc. (Essex Junction, VT, USA); Pierce co-immunoprecipitation kit (26149) from Thermo Scientific (Rockford, IL, USA), *Escherichia coli* derived recombinant murine TNFα from R&D Systems (Minneapolis, MN, USA), DC™ Biorad protein assay kit from Biorad (Nenzlingerweg, Switzerland); VECTASHIELD HardSet® Mounting Media with DAPI from Vector Laboratories (Burlingame, CA, USA). Rhodamine phalloidin, reduced mitotracker orange (M7511), IMAGE-iT LIVE Green ROS Detection Kit (I36007), alexa fluor 633 conjugated secondary goat anti-rabbit (A2107) and anti-mouse (A21052) antibodies were purchased from Invitrogen (Carlsbad, CA, USA). Mouse monoclonal Alexa 555 conjugated anti-α-tubulin (05-829X-555), mouse monoclonal β_3 blocking antibody clone LM609 (MAB1976H) and rabbit polyclonal anti-β_3 integrin antibody (AB2984) were from Millipore (Billerica, MA, USA). Rat monoclonal anti-plasminogen/angiostatin (ab61387), rabbit polyclonal anti-angiostatin (ab2904), rabbit polyclonal anti-β actin (ab8227) and mouse monoclonal anti-ATP synthase β

subunit primary antibody (ab5432) were purchased from Abcam (Cambridge, MA, USA). Donkey anti-goat allophyocyanin conjugated secondary antibody (sc-3860), goat anti-mouse β_3 subunit (sc-6627), goat polyclonal anti-angiomotin s-20 (sc-82494), goat polyclonal anti-angiomotin L-16 (sc-82493), rabbit polyclonal anti-phospho hsp-27 ser82 (sc-101700), goat polyclonal anti-hsp-27 (sc-1048), normal rabbit FITC conjugated IgG (sc-2341) and goat TR conjugated anti-mouse IgG1 isotype control (sc-2979) were from Santa Cruz Biotechnology Inc. (Santa Cruz, CA, USA). Rabbit monoclonal anti-phospho p38 MAPK (4511), rabbit monoclonal anti-p38 MAPK (8690), rabbit polyclonal anti-p44/42 (4372), rabbit monoclonal anti-phospho p44/42 MAPK (4370) and rabbit monoclonal IgG1 isotype control antibody (3900) were from New England Biolabs Inc. (Ipswich, MA, USA). Rabbit polyclonal anti-cleaved caspase-3 antibody (IMG 5700) and mouse monoclonal full length or pro and active caspase-3 antibody (IMG-144A) were purchased from Imigenex (San Diego, CA, USA). Mouse monoclonal anti-flotillin-1 (610820) was from BD Biosciences (San Jose, CA, USA). Secondary anti-rat, anti-mouse, anti-goat and anti-rabbit HRP (horseradish peroxidase) conjugated antibodies for immunoblotting were purchased from Dako, Denmark. All other chemicals, if not specified, were purchased from Sigma Chemicals.

Animal care ethics and human research ethics

All the animals and protocols (protocol number 20070065) were approved by the Research Ethics Board of the University of Saskatchewan, Saskatoon, Canada and complied with Canadian Council in Animal Care in Science guidelines (CCAC). Male C57BL/6 mice were procured from the Animal Resource Centre and housed at the Animal Care Unit at the University of Saskatchewan. The study of neutrophils from healthy human volunteers was approved under protocol Bio number 10–103 and informed consent was obtained from all subjects.

FITC conjugation of angiostatin

FluoroTag kit from Sigma was utilized for angiostatin conjugation to FITC in order to visualize angiostatin in neutrophils. An F/P ratio (i.e., FITC to protein ratio) of 4:1 was achieved after conjugation with a final FITC–angiostatin concentration of 26.7 μg/ml according to small-scale production protocol. The extinction coefficient of unconjugated angiostatin as per the manufacturer's data sheet is 1.74 at 1 mg/ml.

Isolation of mice and human neutrophils

Briefly, peripheral blood was withdrawn by cardiac puncture after ketamine/xylazine anaesthesia from mice and from the intercubital vein of healthy humans. Blood was carefully overlayed onto a discontinuous gradient of Histopaque-1119, 1083 and 1077 according to an established protocol (Nuzzi et al. 2007). After centrifugation at 700*g*, the neutrophil rich layer was aspirated at the interface of Histopaque 1119 and 1083. RBCs were lyzed with ammonium-chloride–potassium (Gibco® ACK) lysing buffer for 3 min for mice or subjected to cold hypotonic lysis in the case of human blood. The washed neutrophil pellet was used for further experiments. The procedure yielded >95 % viable neutrophils upon trypan blue exclusion and staining cytospins for differential leukocyte count.

Confocal microscopy

Confocal images were taken using Leica TCS SP5 (Germany). Images were acquired using a 63X/1.20 oil objective (Leica Plan Apochromat). Neutrophils were equilibrated for 1 h before subjecting them to pre-treatment with PBS, 12.5 μg/ml ANG/FITC-ANG, 500 nMol/l SB230963, 1 μMol/l U0126, or 100 μM cytochalasin D for 30 min. Neutrophils were stimulated with 1 μM fMLP for 1 min, or 1 μg/ml LPS for 30 min, 4 h, or 8 h to either initiate formation of leading edges, or stimulate MAPKinases or caspase-3 cleavage, respectively. Thereafter, the neutrophils were fixed with paraformaldehyde, permeabilized with saponin for 15 min and stained with the respective tagging dyes such as rhodamine phalloidin or reduced mitotracker. In the case of immunofluorescence, neutrophils were adhered to 12 mm circle coverslips coated with fetal bovine serum (FBS) or vitronectin for 5 min. Lipid rafts were depleted by 1 mM methyl-β-cyclodextrin (MCD) for 30 min, whereas 60 μg/ml cholesterol was added for 30 min following MCD treatment to reverse MCD disrupted lipid rafts. Neutrophils were fixed with either 0.7 % glutaraldehyde for 15 min for tubulin only staining or ice-cold methanol for 5 min for multiple protein staining and proceeded for standard immunofluorescence labeling (Allen 2007; Nuzzi et al. 2007). Briefly, the cells were permeabilized with saponin for 15 min, except after methanol fixation, washed with PBS, blocked with 3 % BSA for 1 h, incubated with corresponding primary antibody or isotype controls overnight at 4 °C followed by PBS washes. The secondary antibody was incubated for 1 h and washed with PBS (Allen 2007). To avoid auto-fluorescence from glutaraldehyde, during the tubulin-only staining, the cells were subjected to reduction with 1.5 mg/ml $NaBH_4$ for 30 min just before the blocking step during tubulin staining. The following are the various dilutions of antibodies used: anti-tubulin 1:100, anti-angiomotin 1:100, anti-p-hsp-27 1:100, anti-p-p38MAPK 1:500, anti-p-p44/42 MAPK 1:300, anti-activated caspase-3 1:200, anti-ATP synthase β 1:200. The slides were mounted with VECTASHIELD HardSet® mounting medium that contained DAPI for identification of nuclear morphology.

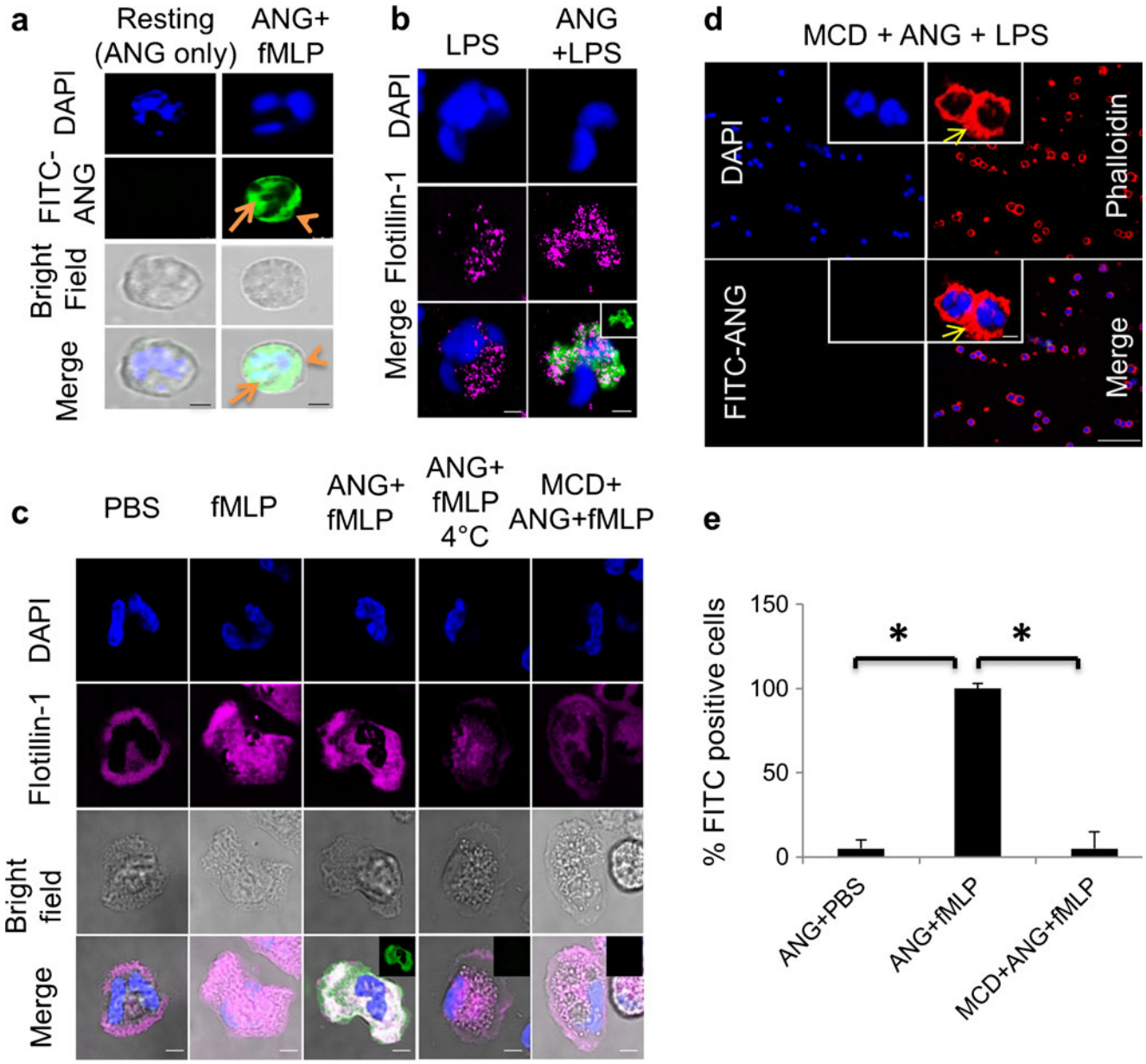

Fig. 1 Uptake of FITC tagged angiostatin in neutrophils and the role of lipid rafts. **a** Localization of FITC tagged angiostatin (*FITC-ANG*) in resting and fMLP activated neutrophils. Suspended mouse neutrophils (0.8×10^6 cells/ml) were pretreated with PBS or 12.5 μg/ml FITC-ANG for 30 min and then treated with PBS or 1 μM fMLP for 1 min. Cells were fixed with 4 % paraformaldehyde for 15 min before making cytospin slides and then coverslipped using hard-set DAPI mounting media ($n=3$). Note the presence of FITC-ANG (in *green*) in the fMLP activated neutrophils only, as indicated by the *arrow* and *arrowhead*. The images are a compilation of the cross-section of the cell. *Bar* = 2.5 μm **b**, **c** Lipid raft dependent uptake of angiostatin. Immunofluorescence of flotillin-1 (in *fuschia*) and FITC-ANG (in *green*, shown as *insets* in the corresponding merge panels) in **b** 1 μg/ml LPS (30 min) and **c** 1 μM fMLP (1 min) stimulated human neutrophils (0.8×10^6 cells/ml) adhered on FBS-coated coverslips ($n=3$). FITC-ANG distributes in a similar way as lipid raft marker, flotillin-1, in activated neutrophils. The uptake of ANG is blocked under cold conditions. MCD treatment inhibited angiostatin uptake and altered flotillin-1 distribution. Note that the merge for the angiostatin treatment groups show the merge of FITC-ANG (*green*) in addition to DAPI (*blue*), flotillin-1 (*fuschia*) and bright-field panels. The bright-field as well as the merge panels depict cell morphology. Angiostatin is represented as ANG and FITC-ANG represents FITC conjugated angiostatin. The images are a compilation of the cross-section of the cell. *Bar* = 2.5 μm. **d** Localization of Alexa 555 phalloidin for actin staining (in *red*) and FITC-ANG (in *green*) in 1 μM fMLP (1 min) stimulated human neutrophils (0.8×10^6 cells/ml) pretreated with 1 mM β methyl cyclodextrin (MCD) adhered on FBS-coated coverslips ($n=3$). MCD treatment abolished uptake of FITC-ANG and induced cortical actin aggregation and leading edge formation. *Arrows* indicate leading edge. Angiostatin is represented as ANG and FITC-ANG represents FITC conjugated angiostatin. The images are a compilation of the cross-section of the cell. *Bar* = 2 μm for the magnified views; 50 μm for the wide-field. **e** Quantification of FITC positive cells, represented as percent FITC positive cells, in resting (ANG+PBS), ANG+ fMLP and MCD pre-treated followed by angiostatin and fMLP treatment. Angiostatin is taken up by nearly 100 % of fMLP activated neutrophils, to suggest wide-spread lipid-raft dependent phenomenon. *$p<0.05$

For the ROS assay, human neutrophils were either pre-treated with 12.5 μg/ml angiostatin for 30 min, followed by 1 μg/ml LPS for 30 min, or the 30 min treatment with 1 μg/ml LPS was followed by 12.5 μg/ml angiostatin post-treatment for 30 min. After the required treatments, the cells were incubated with the ROS detection dye for 30 min more before coverslipping and confocal imaging.

Apoptotic potential of angiostatin was evaluated by routine light microscopy and immunofluorescence and immunoblotting for activated caspase-3. Human neutrophils were either incubated with 12.5 μg/ml ANG for 30 min followed by LPS 1 μg/ml incubations for varying time periods ranging from 2, 4, 6, 8, 10, 12, 14, to 16 h, or 1 μg/ml LPS was incubated for 2 h followed by 4 h ANG treatment.

Western blots

Isolated human neutrophils (5×10^6 cells/ml) were subjected to a 30-min treatment with vehicle, angiostatin (ANG), SB230963, or U0126 before activating them with 1 μg/ml LPS for 30 min. The reaction was terminated by adding cold lysis buffer followed by extraction and centrifugation. The protein concentration was measured in neutrophil lysates by the DC™ Biorad protein assay kit. Equal protein was loaded across groups and subjected to electrophoresis in 12 % SDS-PAGE (180 V), transferred onto nitrocellulose membrane (100 V, 60 min.), blocked with 5 % BSA-0.1 % PBST and immunoblotted for phosphorylated (p-) p38 MAPK (1:1000), p44/42 MAPK (1:1000), total p38 MAPK (1:1000), total p44/42 MAPK (1:1000) p-hsp-27 (1:200), total hsp-27 (1:200), cleaved caspase-3 (1:1000) or full-length (pro and active) caspase-3 (1:500). Membranes were washed with 2.5 % BSA-0.05 % PBST and developed with chemiluminescence GE ECL blot detection reagent.

Co-immunoprecipitation of angiostatin and other proteins

Human neutrophils were treated with ANG only, ANG+fMLP and MCD+ANG+fMLP. Thereafter, they were subjected to lysis with RIPA buffer in the presence of protease and phosphatase inhibitor cocktails and PMSF for 15 min. After a freeze thaw, the samples were centrifuged at 40,000*g* for 30 min at 4 °C and the supernatants were incubated overnight with amino-coupled rat monoclonal anti-plasminogen antibody (10 μg/ml) resin spin columns. Control agarose column was run as a negative control. The protein complex was eluted by boiling with 0.5 % SDS at 95 °C for 5 min. Antibody coupling, column flow-through after sample incubation and elution of protein complex were evaluated for protein concentration through A_{280} absorbance readings (Nanodrop, Fisher Scientific). The protein complex was blotted with the alternative angiostatin antibody (rabbit polyclonal anti-angiostatin antibody), $\alpha_v\beta_3$ integrin (1:1000), angiomotin (1:200), ATP synthase beta subunit (ATP-β) (1:1000), phosphorylated hsp-27 (p-hsp-27) (1:200) and flotillin-1(1:1000).

Intravital cremaster muscle microscopy

To evaluate the effects of ANG on leukocyte adhesion and emigration in vivo, we performed intravital microscopy of the cremaster muscle. Mice were divided into four groups: negative control saline treated ($n=10$), positive control TNFα treated ($n=9$), angiostatin (ANG) only treated ($n=5$) and TNFα+ANG treated ($n=5$).

Mouse recombinant TNFα was injected intrascrotally at a concentration of 0.5 μg/0.05 ml, 3 h before recording. For the TNFα+ANG group, ANG was employed along with TNFα at a dose of 260 μg/mice intrascrotally in a 0.1 ml volume. We used a higher dose of angiostatin because the glycosylated angiostatin used in our experiments, reportedly, has a lower potency in inhibition of endothelial cell proliferation than recombinant angiostatin (Warejcka and Twining 2005). Mice were anaesthetized at a dose of 100 mg/kg ketamine+10 mg/kg xylazine intraperitoneally. The cremaster muscle was carefully exteriorized to avoid activation and tied onto a custom-made cremaster board. The muscle was neither stretched too far nor was it let loose on the stage. After 30 min stabilization, an unbranched post-capillary venule of 25–40 μm diameter was recorded for 5 min at 4.0, 4.5 and 5.0 h time points after specific treatment. An infra-red lamp maintained the body temperature in case of any anaesthetic-induced hypothermia. During the entire experiment, the muscle was superfused with bicarbonate buffer continuously bubbled with air to maintain a pH of 7.4. A BX51 Olympus microscope with a Gibraltar stage was utilized for capturing brightfield images with 10× and 20× objectives coupled to Canon high-definition digital video recording. At the end of the experiment, heparinized peripheral blood was withdrawn by cardiac puncture for total and differential leukocyte counts and cremaster tissue was fixed in 4 % paraformaldehyde for H&E staining.

For image analysis, the recorded video sequences were projected onto a monitor and analyzed off-line for rolling flux (cells/min), rolling velocity (μm/s), adherent cells per 100 μm vessel segment length and emigrated cells per 100 μm vessel length that included any cells that had emigrated below or above the vessel in the cremaster preparation. Rolling flux is described as the average number of leukocytes crossing a fixed reference line, perpendicular to the axis of flow, in 1 min. Rolling velocity is calculated by measuring the time required for the first 20 rolling leukocytes to cross a distance of 100 μm along the vessel. Adhesion is defined as the number of leukocytes adhering to the vessel wall for a minimum of 30 s within a vessel segment of 100 μm in length. Emigration is defined as the number of cells that are observed above and below the vessel at 20×, in the neighbouring interstitial space, within the field of observation.

Cremaster muscle myeloperoxidase (MPO) assay

At the end of the intravital recording, the second cremaster muscle was snap frozen and stored at −80 °C for MPO assay. Cremaster muscle homogenates were centrifuged in 50 mM HEPES (pH 8.0) at 900 g (3,000 rpm) for 20 min at 4 °C. The pellet was resuspended in 0.5 % CTAC (cetyl trimethylammonium chloride) solution and rehomogenized. MPO colorimetric assay was performed (Schierwagen et al. 1990) using 3,3′,5,5′-tetramethylbenzidine as the substrate for H_2O_2 under low pH conditions. Results were expressed as MPO units per mg muscle tissue.

Statistical analysis

All quantitative data are expressed as means±SEMs. The Shapiro–Wilk test was employed for assessing normality of data and equivalence of variance within groups was ascertained by Barlett's test utilizing Stata/SE 10.0 software (Stata Corp., College Station, TX, USA). Quantitative data across multiple groups were analyzed by application of one-way ANOVA followed by Bonferroni's all group comparison and unpaired *t*-test to assess differences between two groups utilizing Graphpad software. We established a p level of 0.05 to establish statistical difference.

Results

Angiostatin is internalized by activated neutrophils in lipid raft dependent fashion

Immunolocalization of angiostatin to visualize its cellular interaction and uptake is nearly impossible because the available angiostatin antibodies react with plasminogen and other angiostatin-like fragments too. Therefore, we conjugated angiostatin to FITC to directly demonstrate surface and cytosolic localization of angiostatin in the fMLP-activated but not in resting neutrophils (Fig. 1a and c) or cold fMLP-activated neutrophils incubated at 4 °C (Fig. 1c). Lipid rafts are cell signalling and endocytic membrane platforms (Fabbri et al. 2005; Singh et al. 2010; Tuluc et al. 2003). We found that FBS adhered fMLP-stimulated human neutrophils endocytose angiostatin in a lipid raft dependent fashion, because angiostatin uptake was disrupted with MCD treatment (Figs. 1c, d, e and 2a) and the uptake was restored with the addition of cholesterol to MCD-treated neutrophils (Fig. 2a).

We further examined the role of lipid rafts in the uptake of FITC–angiostatin in normal and activated neutrophils through localization of flotillin-1. Flotillin-1 shows distribution profiles similar to FITC-angiostatin in LPS-activated (Fig. 1b) or fMLP-activated (Fig. 1c) human neutrophils to allude to a role for lipid rafts in endocytosis of angiostatin. Flotillin-1 expression as well as angiostatin uptake was disrupted when fMLP-activated neutrophils were incubated at 4 °C (Fig. 1c) or treated with MCD (Fig. 1c). The functional role of lipid rafts in the uptake of FITC-angiostatin in human neutrophils was further shown by inhibition of FITC-angiostatin uptake and restoration of actin aggregation in fMLP-activated neutrophils upon pre-incubation with 1 mM MCD to disrupt their lipid rafts (Fig. 1d). Upon counting the number of FITC positive cells in the three groups, it is clear that the phenomenon is widespread in fMLP-activated neutrophils (Fig. 1e). Isotype controls were performed for all the antibodies used in the immunofluorescence experiments and we did not observe any non-specific reactivity for any of the isotypes (Suppl. Fig. 1a).

Fig. 2 Localization of β_3 integrin subunit in angiostatin pretreated fMLP activated neutrophils. **a** Angiostatin is internalized by activated neutrophils in a lipid raft dependent fashion, as indicated by lack of its uptake in lipid raft disrupted neutrophils and reversal after cholesterol treatment. Localization of β_3 integrin subunit (in *red*) and FITC-ANG (in *green*, shown as *insets* in the corresponding merge panels) in PBS or 1 μM fMLP (1 min) stimulated human neutrophils (0.8×10^6 cells/ml) adhered on FBS coated coverslips ($n=3$). Note polarized distribution of β_3 integrin upon fMLP treatment is altered in ANG+fMLP cells. Integrin β_3 distribution in ANG+fMLP cells is disrupted when pretreated with MCD and is reversed after cholesterol (CH) treatment. *Green arrows* indicate the polarized distribution of β_3 integrin subunit in the fMLP group. Please note that the merge for the last three treatment groups show the merge of FITC-ANG (*green*) in addition to DAPI (*blue*), β_3 integrin subunit (*red*) and bright-field. The bright-field as well as the merge panel depict cell morphology. Fluorescent intensity distributions (*FID*) of representative β_3 integrin subunit and FITC-ANG images are shown by *red and green histograms*, respectively. Angiostatin is represented as ANG and FITC-ANG represents FITC conjugated angiostatin. The images are a compilation of the cross-section of the cell. *Bar*=75 μm for wide-field views; 5 μm for the magnified views. **b** Angiostatin abolishes formation of polarized edges in response to fMLP in human neutrophils. Localization of Alexa 555 phalloidin for actin (in *red*) in PBS or 1 μM fMLP (1 min) stimulated human neutrophils (0.8×10^6 cells/ml) adhered on FBS-coated coverslips ($n=3$). fMLP clearly forms an actin-rich leading edge (as marked by the *arrow*). Note attenuation of polarized head in fMLP incubated cells treated with 12.5 μg/ml ANG. LM609 does not affect resting neutrophils. Pre-treatment of fMLP activated neutrophils with LM609 to block the integrin β_3 shows relatively less deformed cells, which are still able to form the leading edge (marked by *arrow*). ANG could not abolish aggregation in LM609 (1:100 dilution) pretreated neutrophils. *Arrows* indicate actin aggregation. Angiostatin is represented as ANG. The images are a compilation of the cross-section of the cell. *Bar*=25 μm for the wide-field views; 2.5 μm for magnified views

Angiostatin abolishes formation of polarized edges and alters β_3 integrin distribution in response to fMLP in neutrophils

Because chemotaxis involves formation of a polarized edges, often referred to as pseudopod at the leading edge and uropod at the trailing edge (Insall 2010), we examined the cytoskeletal dynamics in fMLP-activated mouse and

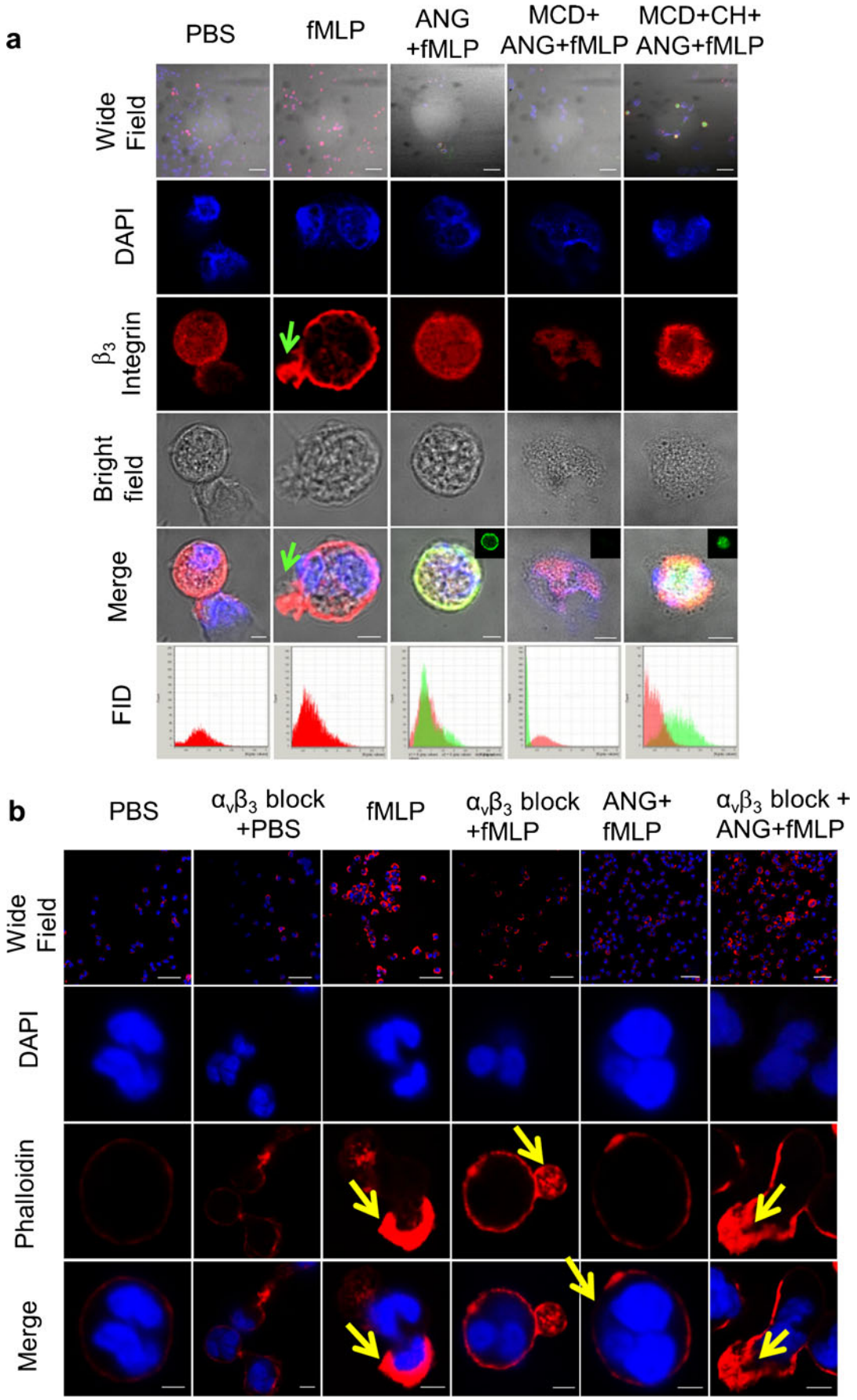
a
PBS
fMLP
ANG +fMLP
MCD+ ANG+fMLP
MCD+CH+ ANG+fMLP
Wide Field
DAPI
β3 Integrin
Bright field
Merge
FID
b
PBS
αvβ3 block +PBS
fMLP
αvβ3 block +fMLP
ANG+ fMLP
αvβ3 block + ANG+fMLP
Wide Field
DAPI
Phalloidin
Merge

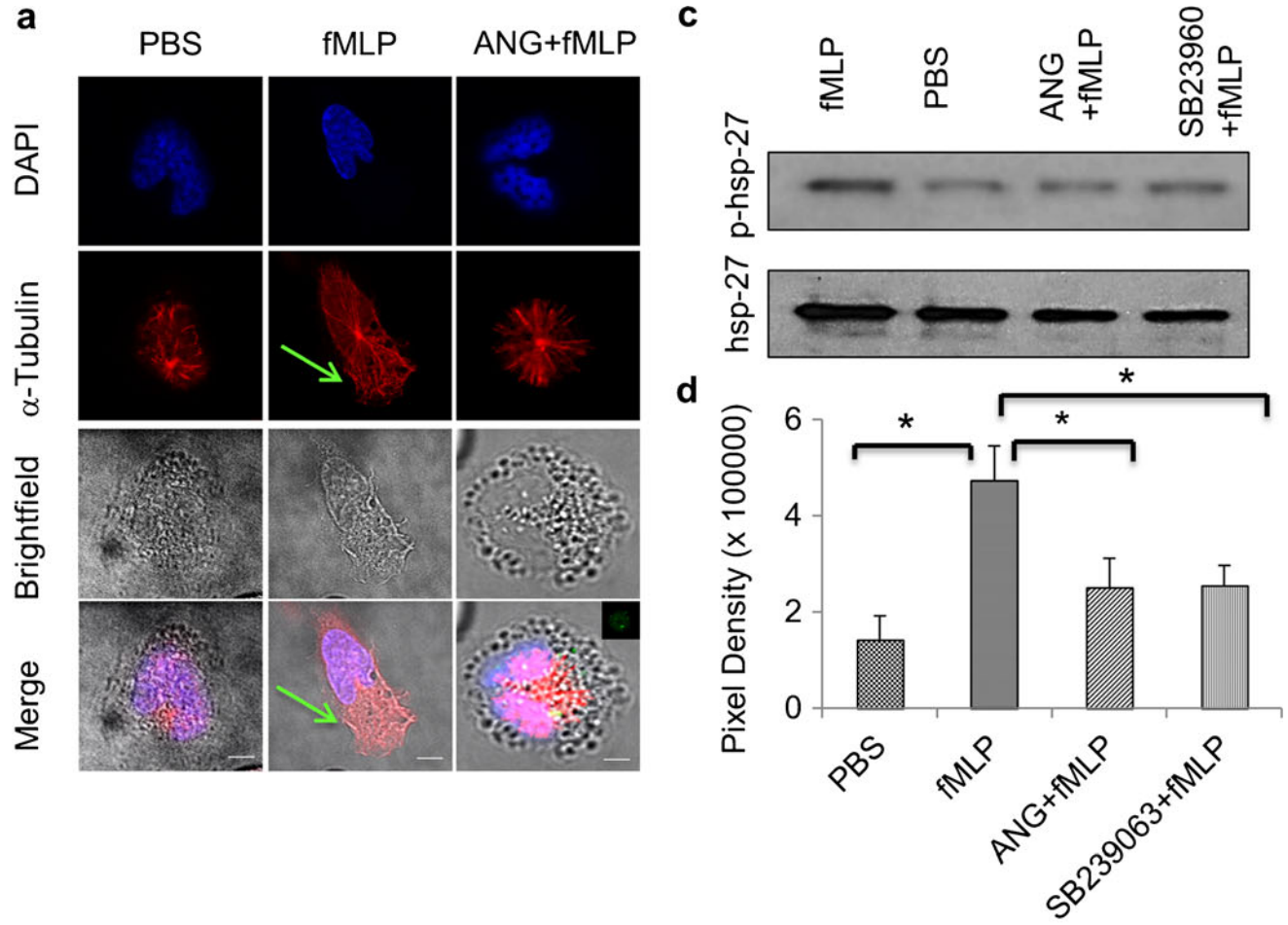
a
PBS
fMLP
ANG+fMLP
DAPI
α-Tubulin
Brightfield
Merge
c
fMLP
PBS
ANG +fMLP
SB23960 +fMLP
p-hsp-27
hsp-27
d
Pixel Density (x 100000)
6
4
2
0
*
*
*
PBS
fMLP
ANG+fMLP
SB239063+fMLP

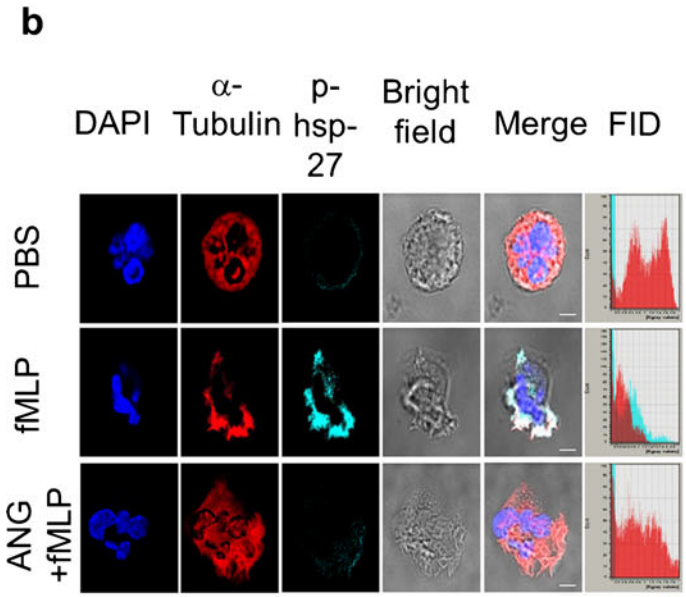
b
DAPI
α-Tubulin
p-hsp-27
Bright field
Merge
FID
PBS
fMLP
ANG +fMLP

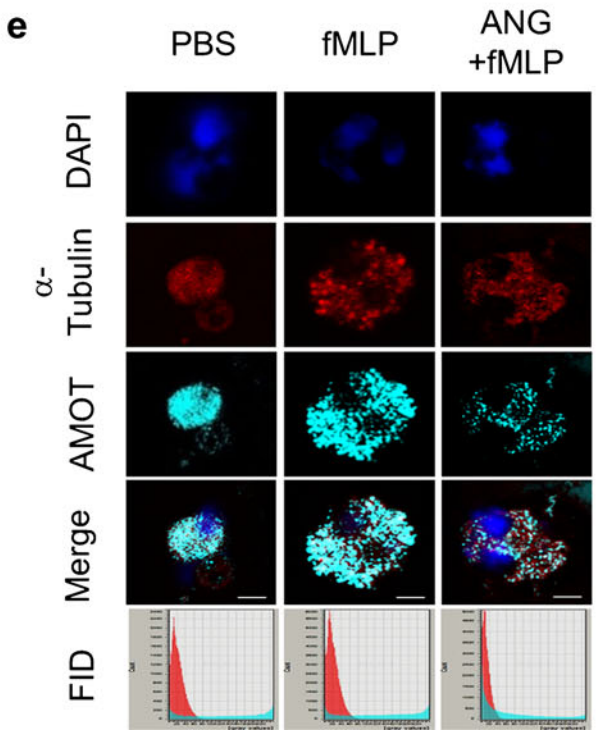
e
PBS
fMLP
ANG +fMLP
DAPI
α-Tubulin
AMOT
Merge
FID

◀ **Fig. 3** Microtubule stabilization by angiostatin. **a** Angiostatin stabilizes and co-localizes with the microtubule network in fMLP-stimulated neutrophils. Localization of α-tubulin (in *red*) and FITC-ANG (in *green*, shown as *inset* in the corresponding merge panel) in PBS or 1 μM fMLP (1 min) stimulated human neutrophils (0.8×10^6 cells/ml) adhered on FBS-coated coverslips. Cells were fixed for 30 min in 0.7 % glutaraldehyde, followed by reduction with 1.5 mg/ml $NaBH_4$ to avoid auto-fluorescence and allow clear visualization of the tubulin network. Note stabilization of tubulin network with 12.5 μg/ml ANG incubated cells. *Arrows* indicate destabilized α-tubulin ($n=3$). Please note that the merge for the last treatment group, i.e., ANG+fMLP shows the merge of DAPI (*blue*) and α-tubulin (*red*) and FITC-ANG (*green*). The bright-field as well as the merge panel depict cell morphology. Angiostatin is represented as ANG and FITC-ANG represents FITC conjugated angiostatin. The images are a compilation of the cross-section of the cell. *Bar*=5 μm. **b** Immunofluorescence of phosphorylated hsp-27 (p-hsp-27) (in *cyan*) and α-tubulin (in *red*) in fMLP (1 min) stimulated human neutrophils (0.8×10^6 cells/ml) adhered on FBS-coated coverslips. Cells were fixed for 5 min in ice-cold methanol to permeabilize and immunostain tubulin as well as php-27. The bright-field as well as the merge panels depict cell morphology. Note stabilization of tubulin network with 12.5 μg/ml ANG+fMLP treated neutrophils ($n=3$). Fluorescent intensity distributions (*FID*) of representative p-hsp-27 and α-tubulin are shown by *cyan and red histograms*, respectively. Angiostatin is represented as ANG. The images are a compilation of the cross-section of the cell. *Bar*=2 μm. **c** Representative western blots showing expression of p-hsp-27 and hsp-27 in human neutrophil lysates subjected to SDS electrophoresis ($n=3$). Human neutrophils (5×10^6/ml) were activated with 1 μM fMLP (1 min). Angiostatin is represented as ANG. **d** Average pixel densitometry of phsp-27 with hsp-27 as control from three separate western blots. Note attenuation of phsp-27 in 12.5 μg/ml ANG as well as 500nM SB239063 pretreated neutrophils activated with fMLP. *$p<0.05$. **e** Immunofluorescence of angiomotin (AMOT) (in *cyan*) and α-tubulin (in *red*) in 1 μM fMLP (1 min) stimulated human neutrophils (0.8×10^6 cells/ml) adhered on FBS-coated coverslips. Cells were fixed for 5 min in ice-cold methanol to permeabilize and immunostain tubulin as well as php-27. Note stabilization of tubulin network and altered angiomotin distribution in ANG+fMLP treated cells ($n=3$). Fluorescent intensity distributions (*FID*) of representative angiomotin and α-tubulin are shown by *cyan and red histograms*, respectively. Angiostatin is represented as ANG. The images are a compilation of the cross-section of the cell. *Bar*=2 μm

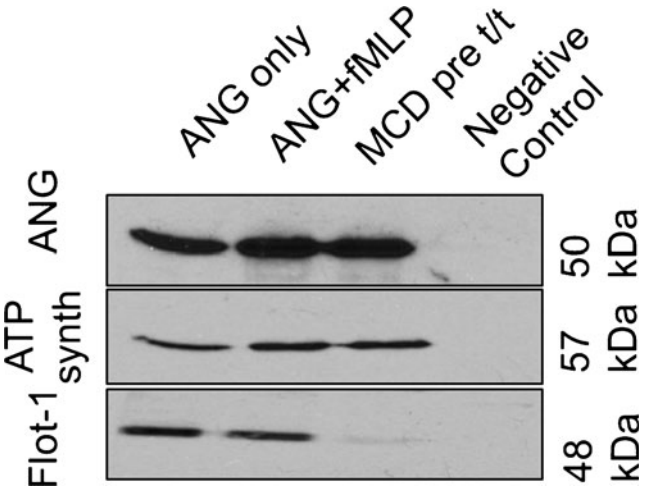

Fig. 4 Angiostatin co-immunoprecipitation with interacting proteins. Anti-rat monoclonal plasminogen/angiostatin antibody (10 μg/reaction) was linked to activated agarose beads through amino linkage. One reaction had control agarose beads that served as the negative control. Whole human peripheral blood neutrophil lysates (5×10^7 cells/treatment) were prepared from three different treatment groups: ANG only, ANG+fMLP treated and MCD pretreated ANG+fMLP group. The lysates were incubated overnight with antibody coupled beads as well as with the negative control beads at 4 °C. The complex was thoroughly washed with modified Dulbecco's wash buffer and eluted by boiling the beads with 50 μl of 0.5 % SDS at 95–100 °C for 5 min. The eluted complex was subjected to electrophoresis with 12 % SDS-PAGE. PVDF membrane with transferred proteins was thereafter immunoblotted overnight with either rabbit polyclonal anti-angiostatin antibody (1:1000), rat monoclonal anti-plasminogen/angiostatin antibody (1:1000), mouse monoclonal anti-ATP synthase antibody (1:1000), or mouse monoclonal anti-flotillin-1 (flot-1) antibody (1:1000). The blots are representative of three separate experiments

human neutrophils. Angiostatin pre-treatment prevented reorganization of actin filaments and formation of a polarized head in mouse (Suppl. Fig. 1b) and human neutrophils (Fig. 2b). Mouse neutrophils treated with cytochalasin D, a potent inhibitor of actin polymerization, also failed to develop the polarized edge (Suppl. Fig. 1b) in response to fMLP. β_3 integrins, a receptor of angiostatin, localize in a Ca^{2+}-dependent manner to the leading edge during chemotaxis of neutrophils on vitronectin (Hendey et al. 1996; Lawson and Maxfield 1995). β_3 integrin distribution is also altered by angiostatin as well as MCD treatment of fMLP-activated neutrophils (Fig. 2a). The altered morphology of β_3 integrin was restored through addition of cholesterol to MCD-treated fMLP-activated human neutrophils (Fig. 2a). Moreover, the fluorescent intensity histogram for β_3 integrin superimposes with angiostatin (Fig. 2a). Because ours and earlier data show that angiostatin binds with β_3 integrin on neutrophils (Tarui et al. 2001), we treated human neutrophils with a humanized function-blocking $\alpha_v\beta_3$ antibody (clone LM609) to study whether angiostatin is acting via the integrin. LM609, per se, did not affect the actin dynamics (Fig. 2a). Treatment of fMLP-activated neutrophils with LM609 did not prevent actin aggregation. However, it did prevent whole cell deformation and reduced the intensity of phalloidin staining in the leading edge that is normally observed in response to fMLP (Fig. 2b). Intriguingly, treatment of fMLP-treated human neutrophils with angiostatin and LM609 antibody, in contrast to angiostatin alone, did not prevent formation of pseudopods (Fig. 2b).

Angiostatin stabilizes the microtubule network in fMLP-stimulated neutrophils

Microtubules are destabilized in fMLP-stimulated neutrophils (Fig. 3a) (Eddy et al. 2002). Angiostatin stabilized α-tubulin

(tubulin) in fMLP-stimulated human neutrophils (Fig. 3a, b and e). Phosphorylated heat shock protein-27 (p-hsp-27) (Dudani et al. 2007) and angiomotin (Wells et al. 2006) are known to interact with angiostatin. Resting neutrophils showed little, if any, p-hsp-27 staining, as indicated by low fluorescence intensities in PBS-treated neutrophils (Fig. 3b and Suppl. Fig. 1c). As reported by others (Hino et al. 2000; Hino and Hosoya 2003; Jog et al. 2007), we observed similar distribution profiles of p-hsp-27 with tubulin in resting as well as fMLP-stimulated human neutrophils and that fMLP produces a strong polarization of p-hsp-27 and tubulin (Fig. 3b and Suppl. Fig. 1c), as indicated by the overlapping regions of fluorescence intensity histograms of p-hsp-27 and tubulin (Fig. 3b). Angiostatin treatment reduced the morphological expression for p-hsp-27 as depicted in the near basal intensity values in the ANG+fMLP group (Fig. 3b), which was confirmed with western blots (Fig. 3c and d) and stabilized the tubulin network in fMLP-stimulated human neutrophils (Fig. 3b and Suppl. Fig. 1c). The p38 MAPK inhibitor, SB239063, effectively blocked the phosphorylation of hsp-27, as indicated in Western blot quantification (Fig. 3c and d). Total hsp-27 protein remained unaltered across groups. Angiomotin is recognized as an angiostatin-binding protein, and is widely expressed in endothelial and epithelial cells, where it has been shown to interact with cdc-42 Rho GTPase activating protein (GAP), Rich1(Gagne et al. 2009) and its transcript is expressed in neutrophils (Benelli et al. 2002). We found that angiomotin expression in neutrophils was similar to the tubulin network in resting as well as fMLP-treated human neutrophils (Fig. 3e and Suppl. Fig. 1d). fMLP induces polarization of angiomotin as well as the alpha-tubulin (Fig. 3e). Angiostatin pretreatment stabilized the tubulin and appeared to reduce expression of angiomotin (Fig. 3e). Collectively, angiostatin's inhibitory effects on p-hsp-27, alpha-tubulin and angiomotin may block chemotaxis and affect maintenance of cell shape in activated neutrophils.

Angiostatin co-immunoprecipitates with integrin β_3, ATP synthase-beta subunit and flotillin-1

We performed co-immunoprecipitation to confirm co-localization of proteins examined in our experiments. While no bands were observed in the negative control agarose spin columns that were disabled for amino-coupling of plasminogen/angiostatin antibody (Fig. 4), we confirmed the presence of angiostatin by blotting with rabbit anti-angiostatin antibody that recognizes internal *kringle* fragments, as well as with rat anti-plasminogen/angiostatin antibody raised against whole plasminogen as the immunogen. The data show that 57 kDa ATP synthase-β subunit and 48 kDa flotillin-1 bands co-eluted with the immunoprecipitated angiostatin complex (Fig. 4 and Suppl. Fig. 2a). Immunoreactivity for 50 kDa angiostatin as well as 85 kDa integrin β_3 was observed in resting as well as fMLP-activated neutrophils (Suppl. Fig. 2a). While flotillin-1 band was very faint in MCD-treated cell isolates, angiostatin and ATP synthase-β immuno-reactivity was not altered (Fig. 4).

Fig. 5 Effect of angiostatin on neutrophil redox status and F_1F_0 ATP synthase localization. **a** Angiostatin attenuates mitochondrial dye oxidation and attenuates reactive oxygen species (ROS) production. Localization of reduced mitotracker (Red Mito in *red*) in 1 μM fMLP (1 min) stimulated mouse neutrophils (0.8×10^6 cells/ml) in suspension, adhered on fetal bovine serum (FBS)- or vitronectin-coated coverslips. Notice attenuation of mitochondrial activation after 12.5 μg/ml FITC-ANG pre-incubation ($n=3$). Please note that the merge for the last treatment group, i.e., ANG+LPS on vitronectin-coated coverslips shows the merge of DAPI (*blue*), reduced mitotracker (*red*) and FITC-ANG (in *green*, also shown as *inset* in the merge panel). The fluorescence intensity distribution (*FID*) of the region of interest, *ROI*, (*encircled in yellow*) shows overlapping distribution of FITC-ANG and the reduced mitotracker dye in vitronectin-coated LPS activated neutrophils, suggesting their co-localization. Angiostatin is represented as ANG. The images are a compilation of the cross-section of the cell. *Bar* = 2 μm. **b** Immunofluorescence of F_1F_0 ATP synthase β subunit (in *fuschia*) and reduced mitotracker (in *red*) in 1 μg/ml LPS (30 min) stimulated human neutrophils (0.8×10^6 cells/ml) adhered on FBS-,coated coverslips ($n=3$). Note attenuation of fluorescent signal for ATP synthase as well as reduced mitotracker in 12.5 μg/ml ANG incubated cells. *Arrows* indicate expression of ATP synthase. Angiostatin is represented as ANG. The images are a compilation of the cross-section of the cell. *Bar* = 2 μm. **c** Fluorescence intensity quantification of ATP synthase (*fuschia* channel) for PBS, LPS and LPS+ANG treatment groups as indicated in the confocal experiment described above ($n=3$). Average intensities, for the fuschia channel, from 100 neutrophils per slide were measured by Image J software. Angiostatin is represented as ANG. $^*p<0.05$. **d** Representative western blot showing expression of F_1F_0 ATP synthase β subunit in human neutrophil lysates subjected to SDS electrophoresis ($n=3$). Human neutrophils (5×10^6/ml) were treated with PBS, activated with 1 μg/ml LPS (30 min), 12.5 μg/ml ANG+1 μg/ml LPS. Angiostatin is represented as ANG. **e** Average pixel density from three separate western blots depicts the expression of F_1F_0 ATP synthase β subunit.$^*p<0.05$. No significant differences were observed in the expression of ATP synthase across groups. Angiostatin is represented as ANG

Angiostatin inhibits mitochondrial activation and attenuates ROS production

In addition to increased migration into inflamed tissues, activated neutrophils have active mitochondria that cause increased ROS production (Fialkow et al. 2007). Reduced mitotracker dye, which binds to mitochondria in the presence of ROS, stained mitochondria in fMLP or LPS-activated mouse neutrophils in suspension as well as those adhered to fetal bovine serum or vitronectin (Fig. 5a). Angiostatin attenuated the signal for reduced mitotracker dye in suspended or adhered mouse neutrophils treated with LPS or fMLP (Fig. 5a). Mouse neutrophils adhered to vitronectin and stimulated with LPS showed partial co-localization of angiostatin with reduced mitotracker dye, as indicated by the overlapping fluorescence intensity histogram for mitotracker in red and FITC conjugated angiostatin in green (Fig. 5a; Suppl. Mov. 1).

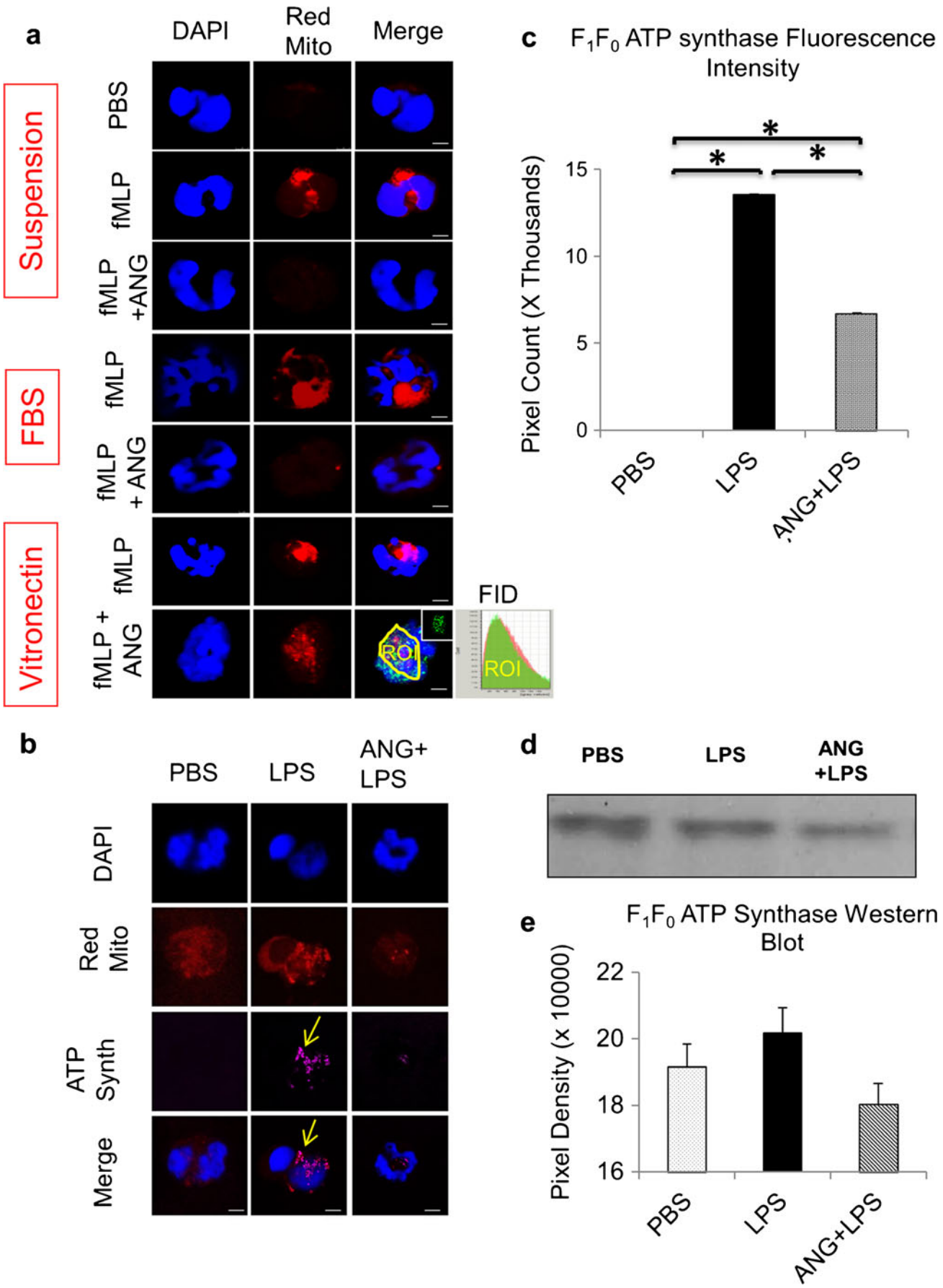
a
DAPI
Red Mito
Merge
Suspension
PBS
fMLP
fMLP +ANG
FBS
fMLP
fMLP + ANG
Vitronectin
fMLP
fMLP + ANG
FID
ROI
ROI
c
F1F0 ATP synthase Fluorescence Intensity
Pixel Count (X Thousands)
15
10
5
0
*
*
*
PBS
LPS
ANG+LPS
b
PBS
LPS
ANG+ LPS
DAPI
Red Mito
ATP Synth
Merge
d
PBS
LPS
ANG +LPS
e
F1F0 ATP Synthase Western Blot
Pixel Density (x 10000)
22
20
18
16
PBS
LPS
ANG+LPS

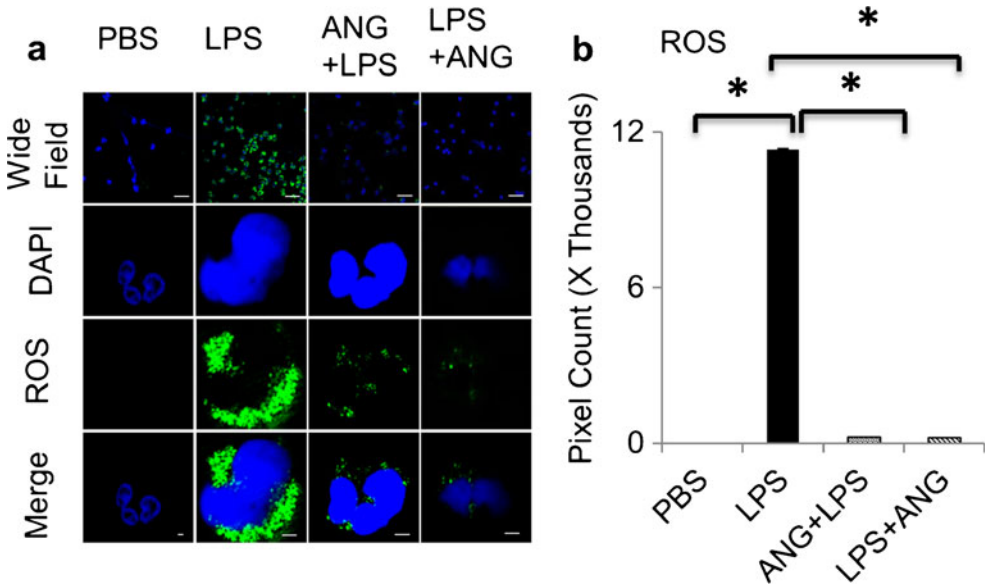

Fig. 6 Inhibition of reactive oxygen species production by angiostatin pre- as well as post-treatment. **a** Localization of reactive oxygen species (ROS) detected by carboxy-H_2 DCFDA (in *green*) in PBS- or LPS-stimulated human neutrophils (0.8×10^6 cells/ml). Neutrophils were either pre-treated with 12.5 μg/ml angiostatin for 30 min, followed by 1 μg/ml LPS for 30 min, or the 30-min treatment with 1 μg/ml LPS was followed by 12.5 μg/ml angiostatin post-treatment for 30 min more. After the required treatments, the cells were incubated with the ROS detection dye for 30 min more before putting cover slips and confocal imaging. Note attenuation of ROS in cells treated with ANG before or after exposure to LPS ($n=3$). Angiostatin is represented as ANG. The images are a compilation of the cross-section of the cell. *Bar* = 2.5 μm for the magnified views; 25 μm for the merged wide-field views. **b** Fluorescence intensity measurements of carboxy-H_2 DCFDA (*green* channel) in PBS, LPS ANG+LPS and LPS+ANG treatment groups, as indicated in the confocal experiment described above ($n=3$). Average intensities, for the green channel, from 100 neutrophils per slide were measured by Image J software. Angiostatin is represented as ANG. *$p<0.05$

Mitochondrial F_1F_0 ATP synthase upon translocation to the plasma membrane is proposed as a receptor for angiostatin (Lee et al. 2009). Angiostatin attenuated F_1F_0 ATP synthase staining in LPS–stimulated human neutrophils (Fig. 5b and c). Western blots of human neutrophil lysates showed no significant differences in the amount of F_1F_0 ATP synthase in PBS-, LPS- or angiostatin+LPS-treated neutrophils (Fig. 5d and e).

Angiostatin attenuated ROS production, which was evaluated with carboxy-H_2DCFDA (5-(and 6-) carboxy-2′,7′-dichlorodihydrofluorescein diacetate), in LPS-treated human neutrophils (Fig. 6a). This finding further confirmed our preceding observation of angiostatin's attenuation of reduced mitotracker dye, which is used to determine the redox status (Fig. 5). Interestingly, ROS production was reduced in neutrophils even when they were activated with LPS prior to angiostatin treatment (Fig. 6a and b). Taken together, these data show that angiostatin inhibits mitochondrial activation and production of ROS in activated neutrophils.

Angiostatin inhibits MAPK signalling in activated neutrophils

We investigated the impact of angiostatin on MAPK because p38 MAPKinase is implicated in cell migration signalling (Niggli 2003; Spisani et al. 2005; Underwood et al. 2000) and p44/42 MAPKinase or ERK1/2 is involved in activation of NADPH oxidase required for generation of ROS (Espinosa et al. 2006; Markvicheva et al. 2010). Mouse as well as human neutrophils activated with LPS showed strong signals for phosphorylated p-p38 (Fig. 7a; Suppl. Fig. 2b) and p-p44/42

Fig. 7 Effect of angiostatin on p38 as well as p44/42 MAPK ▶ phosphorylation in human neutrophils. **a** Angiostatin inhibits MAPK signalling. Immunofluorescence of phosphorylated p38 MAPKinase (p-p38 MAPK) (in *cyan*), actin (in *red*) in PBS- or 1 μg/ml LPS (30 min)-stimulated human neutrophils (0.8×10^6 cells/ml) adhered on FBS-coated coverslips. Note attenuation of the signal in ANG incubated cells. ($n=3$). Angiostatin is represented as ANG. The images are a compilation of the cross-section of the cell. *Bar* = 2 μm. **b** Expression of phosphorylated p38 MAPKinase (p-p38 MAPK) and total p38 MAPK in human neutrophil lysates subjected to SDS electrophoresis. Neutrophils (5×10^6 cells/ml) were activated with 1 μg/ml LPS for 30 min. SB239063 was used as standard p38 MAPK inhibitor. Angiostatin is represented as ANG. **c** Pixel density from three separate western blots depicts the expression of p-p38 MAPK protein. Note attenuation of p-p38MAPK in 12.5 μg/ml ANG as well as 500nM SB239063 pre-treated (30 min.) neutrophils activated with LPS. Angiostatin is represented as ANG. *$p<0.05$. **d** Immunofluorescence of phosphorylated p42/44 MAPKinase (p-p44/42 MAPK) (in *cyan*) and actin (in *red*) in PBS- or LPS (30 min)-stimulated human neutrophils (0.8×10^6 cells/ml) adhered on FBS-coated coverslips. U0126 was used as selective p44/42 MAPK inhibitor. Angiostatin is represented as ANG. The images are a compilation of the cross-section of the cell. *Bar* = 2 μm. **e** Representative western blot showing expression of p-p44/42 MAPK and total p44/42 MAPK protein in human neutrophil lysates subjected to SDS electrophoresis ($n=3$). Neutrophils (5×10^6 cells/ml) were activated with 1 μg/ml LPS for 30 min. Angiostatin is represented as ANG. **f** Average pixel density from three separate western blots depicts the expression of p-p44/42 MAPK protein. Note attenuation of p-p44/42 MAPK in 12.5 μg/ml ANG as well as 1 μM U0126 pre-treated (30 min) neutrophils. Angiostatin is represented as ANG. *$p<0.05$

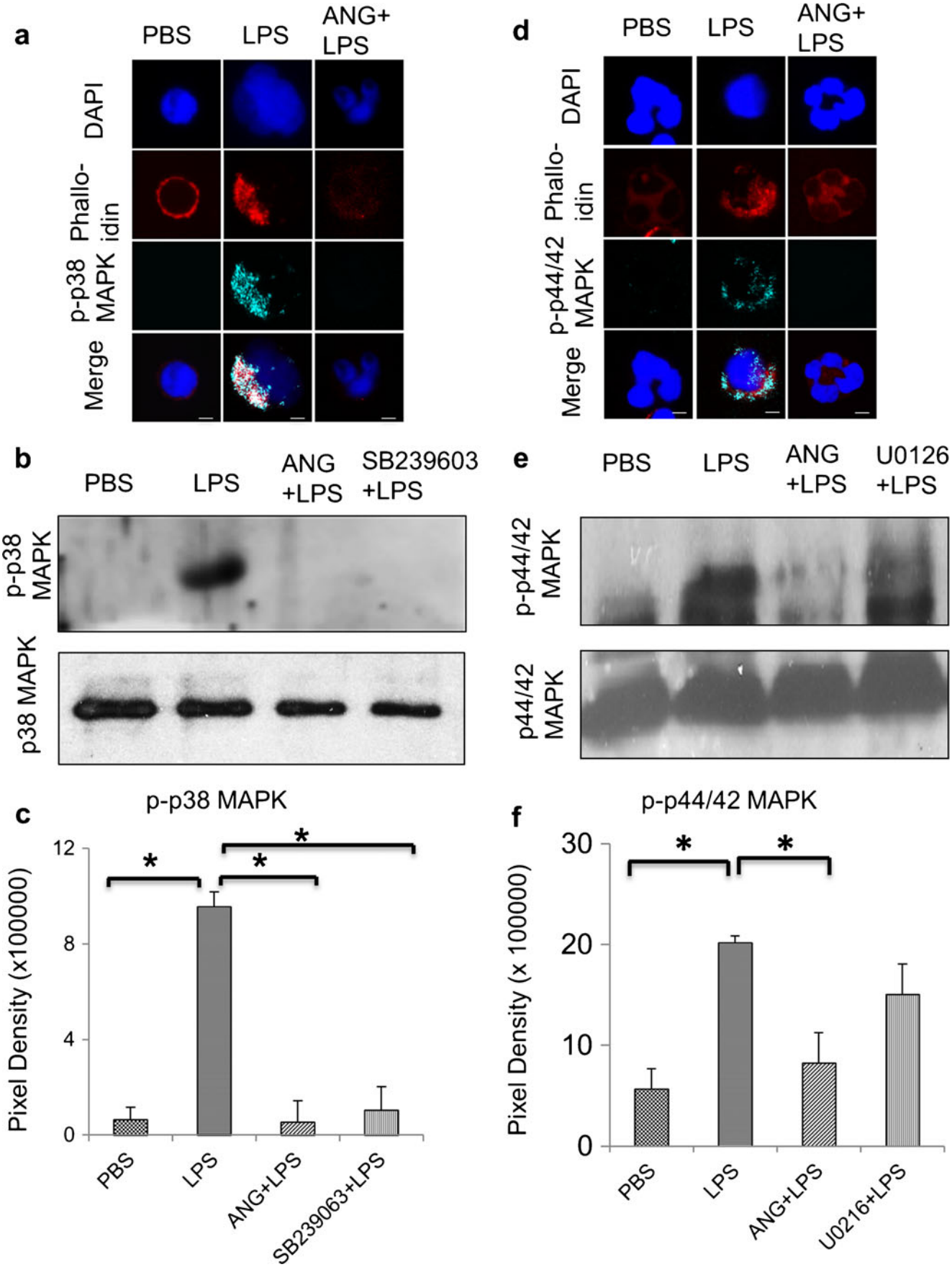
a
PBS
LPS
ANG+ LPS
DAPI
Phallo-idin
p-p38 MAPK
Merge
d
PBS
LPS
ANG+ LPS
DAPI
Phallo-idin
p-p44/42 MAPK
Merge
b
PBS
LPS
ANG +LPS
SB239603 +LPS
p-p38 MAPK
p38 MAPK
e
PBS
LPS
ANG +LPS
U0126 +LPS
p-p44/42 MAPK
p44/42 MAPK
c
p-p38 MAPK
Pixel Density (x100000)
12
8
4
0
*
*
*
PBS
LPS
ANG+LPS
SB239063+LPS
f
p-p44/42 MAPK
Pixel Density (x 100000)
30
20
10
0
*
*
PBS
LPS
ANG+LPS
U0216+LPS

MAPKinases (Fig. 7d; Suppl. Fig. 2c) and angiostatin diminished these signals, as shown with microscopy (Fig. 7a and d; Suppl. Fig. 2b and c) and western blots (Fig. 7b, c, e and f). Similar to angiostatin treatment, the expression of p-p38 and p44/42 MAPKinase was reduced by known inhibitors of p38 and p44/42 MAPK phosphorylation, SB239603 and U0126, respectively, in LPS-stimulated human neutrophils (Fig. 7b, c, e and f). These data show that angiostatin significantly inhibits phosphorylation of p38 MAPK and p44/42 MAPK to induce other downstream effects in neutrophils.

Angiostatin induces apoptosis in LPS-activated human neutrophils

Lastly, we examined the effects of angiostatin on apoptosis in activated human neutrophils because it is known that LPS prolongs neutrophil survival by delaying their constitutive apoptosis (Aoshiba et al. 1999). To determine whether angiostatin induces apoptosis in LPS-activated neutrophils, we incubated human neutrophils with LPS with or without angiostatin pre-treatment and stained them for cleaved caspase-3 as an indicator of apoptosis. LPS treatment suppressed expression of cleaved caspase-3 in human neutrophils compared to PBS-treated neutrophils (Fig. 8a and b). On the other hand, angiostatin treatment of human neutrophils, as early as 4 h, either before or after the LPS treatment, significantly increased the expression of activated caspase-3 compared to both control and LPS-activated neutrophils (Fig. 8a and b). Lysates from respective neutrophil treatments were subjected to SDS-PAGE electrophoresis to confirm confocal data for activated caspase-3 expression. Western blot densitometry performed with full-length caspase-3 as the control showed a significant increase in cleaved caspase-3 protein in human neutrophils treated with angiostatin either before or after incubation with LPS compared to the LPS-only treatment (Fig. 8c and d). Furthermore, the cleaved caspase-3 protein expression was lower in all of the LPS groups compared to the saline-treated human neutrophils (Fig. 8c and d). SB239603, employed as a standard p38 MAPK inhibitor for the western blot experiments, restored the caspase-3 expression to control values in LPS-treated neutrophils (Fig. 8c and d). Finally, we used light microscopy on neutrophil cytospins to morphologically quantify the number of apoptotic cells. The data show that angiostatin treatment of human neutrophils before or after the exposure to LPS caused a significant increase in the numbers of apoptotic cells compared to the LPS-control at all the observed time points and at 4, 6 and 8 h when compared to PBS-treated neutrophils (Fig. 8e and f).

Angiostatin inhibits adhesion and transendothelial migration in TNFα-activated cremaster muscle

To find out whether the in vitro effects of angiostatin on neutrophils translate in vivo, we did intravital microscopic evaluation of effects of angiostatin on recruitment of leukocytes under flow conditions in post-capillary venules in cremaster muscle. The rolling flux was significantly reduced in the TNFα group at all time-points compared to the control groups as well as angiostatin treatment groups (Fig. 9a). Adhesion and emigration was significantly higher in the TNFα group compared to all other groups. The TNFα+ angiostatin treatment group had a significantly higher number of adhered and emigrated cells compared to the saline and angiostatin-only groups but was less when compared to the TNFα group (Fig. 9 c and d). Control groups such as saline or angiostatin only had significantly higher rolling velocity compared to the TNFα or TNFα+angiostatin treatment groups (Fig. 9b). TNFα upregulates chemokine expression and produces acute inflammation in the cremaster muscle with significantly lower rolling flux, velocity and a markedly high index of neutrophil adhesion and emigration (Liu and Kubes 2003; Wong et al. 2010). Angiostatin treatment produces significantly higher rolling flux and velocity and a

Fig. 8 Effect of angiostatin on neutrophil apoptosis **a** Angiostatin induces apoptosis in LPS-activated human neutrophils. Neutrophils were either incubated with 12.5 μg/ml ANG for 30 min followed by LPS 1 μg/ml incubations for varying time periods ranging from 2, 4, 6, 8, 10, 12, 14, to 16 h, or 1 μg/ml LPS was incubated for 2 h followed by 4 h ANG treatment. Immunofluorescence of cleaved caspase-3 (Cleav Casp-3 in cyan) in human neutrophils (0.8×10^6 cells/ml) adhered on FBS-coated coverslips. Note activation of cleaved caspase-3 in cytosol of 12.5 μg/ml ANG pre- and post-LPS treatments ($n=3$). Angiostatin is represented as ANG. The images are a compilation of the cross-section of the cell. *Bar* = 2 μm for magnified views; 25 μm for the wide-field views. **b** Fluorescence intensity measurements of cleaved caspase-3 (*cyan* channel) in PBS, LPS, ANG+LPS and LPS+ANG treatment groups, as indicated in the confocal experiment described above ($n=3$). Average intensities, for the cyan channel, from 100 neutrophils per slide were measured by Image J software. Angiostatin is represented as ANG. *$p<0.05$. **c** Representative western blots showing expression of cleaved caspase-3 (Cleav Casp-3) and full-length (pro and active) caspase-3 (Casp-3) protein in human neutrophil lysates subjected to SDS electrophoresis ($n=3$). Neutrophils (5×10^6 cells/ml) were activated with 1 μg/ml LPS for 30 min. SB239063 was used to selectively block p38 MAPK and used as the control. The levels of total caspase-3 are relatively constant across the groups. Angiostatin is represented as ANG. **d** Average pixel density from three separate western blots depicts the expression of cleaved caspase-3 protein. While all of the LPS-treated groups have lower expression of cleaved caspase-3 compared to PBS control and SB239063 pre-treated neutrophils, both ANG-treated groups have significantly higher cleaved caspase-3 expression compared to LPS-only group. Angiostatin is represented as ANG. *$p<0.05$. **e** Representative light microscopic neutrophil morphology in PBS, LPS ANG+LPS and LPS+ANG treatment groups at 6 h time-point (n=3). **f** Apoptotic neutrophils were identified under a high power oil-field at 2, 4, 6, 8, 10 and 12 h time-points for all the mentioned treatment groups ($n=3$) and counted in ten different fields or a total of 500 neutrophils per slide. Percent apoptosis was then represented across the groups. ANG+LPS and LPS+ANG show a significant increase in the numbers of apoptotic cells compared to the LPS-control at all the time points and 4, 6 and 8 h compared to PBS-treated neutrophils. Values are expressed as mean (% apoptotic cells)±SE from three different experiments. Angiostatin is represented as ANG. *$p<0.05$. *Bar* = 10 μm

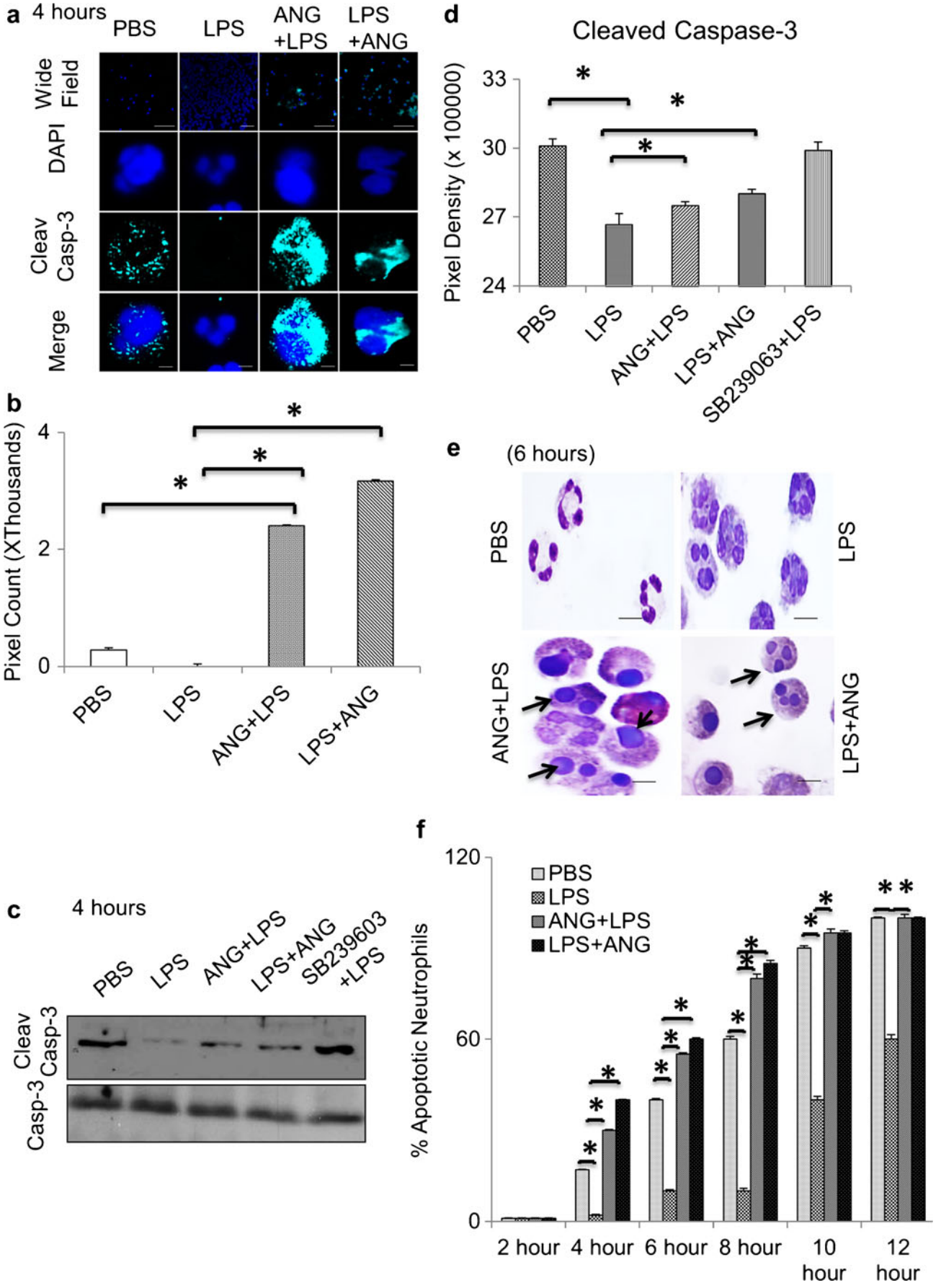
a
4 hours
PBS
LPS
ANG +LPS
LPS +ANG
Wide Field
DAPI
Cleav Casp-3
Merge
b
Pixel Count (XThousands)
0
2
4
PBS
LPS
ANG+LPS
LPS+ANG
c
4 hours
PBS
LPS
ANG+LPS
LPS+ANG
SB239603 +LPS
Cleav Casp-3
Casp-3
d
Cleaved Caspase-3
Pixel Density (x 100000)
24
27
30
33
PBS
LPS
ANG+LPS
LPS+ANG
SB239063+LPS
e
(6 hours)
PBS
LPS
ANG+LPS
LPS+ANG
f
% Apoptotic Neutrophils
0
60
120
PBS
LPS
ANG+LPS
LPS+ANG
2 hour
4 hour
6 hour
8 hour
10 hour
12 hour

significantly lower adhesion and emigration compared to TNFα treatment. H&E data (Fig. 9e) showed reduced recruitment and extravascular migration of neutrophils, to support the off-line video analysis (Suppl. Mov. 2, 3, 4, 5). The dose of TNFα employed in our study did not produce systemic effects, as indicated by similar leukocyte counts in the peripheral blood (Suppl. Table 1).

Angiostatin reduces neutrophil recruitment in TNFα inflamed cremaster muscle

To further determine the effects of angiostatin on neutrophil recruitment into cremaster tissues, we used MPO as a surrogate marker to quantify infiltrated neutrophils. TNFα group has significantly higher MPO compared to the saline, ANG only and TNFα+ANG groups (Fig. 9f).

Discussion

There is a pressing need to identify molecules that modulate neutrophil function and associated tissue damage in various inflammatory diseases. The series of in vitro experiments detailed in this manuscript provide conclusive morphological and molecular data that angiostatin silences activated neutrophils through inhibition of MAPK cell signals, cytoskeletal reorganization, attenuation of ROS formation and induction of activated caspase-3. We also report that neutrophil inhibitory effects translate in vivo as angiostatin inhibits TNFα-induced neutrophil migration in post-capillary venules of cremaster muscle. Because angiostatin is an endogenous protein expressed at augmented levels in inflammation and is produced by neutrophils (Lucas et al. 2002; Scapini et al. 2002), the data open possibilities to exploit angiostatin for therapeutic purposes.

First, we determined that angiostatin does not bind to resting neutrophils but binds to and is endocytozed by fMLP-activated neutrophils. It is challenging to study the localization of angiostatin, because most of the antibodies cross-react with plasminogen. The immuno-reactivity of angiostatin in resting, fMLP-activated and lipid raft-disrupted neutrophil lysates could be due to many reasons. For example, it may be due to binding of native angiostatin in the cytosolic compartments of neutrophils, as evidenced by co-elution of ATP synthase-β in lipid raft-disrupted neutrophils. Also, angiostatin reactivity in neutrophils could be due to microplasmin, another 50 kDa cleavage product, formed after activation of plasminogen to plasmin (Hermel et al. 2010). We overcame the challenge of lack of specific plasminogen/angiostatin antibodies by using FITC conjugation with angiostatin in confocal microscopy. The data also show that angiostatin uptake by activated neutrophils may be an active energy-dependent process, because the uptake was inhibited at 4 °C. It appears that lipid rafts may play a role in the uptake of angiostatin as angiostatin distributed similar to the lipid raft marker, flotillin-1, in LPS- as well as fMLP-stimulated neutrophils. The disruption of lipid rafts as shown by loss of flotillin-1 in confocal microscopy was supported by the coimmuno-precipitation data, and was accompanied by inhibition of uptake of FITC-angiostatin by the neutrophils. The uptake of angiostatin in MCD-treated neutrophils was restored through addition of cholesterol to the experiment set-up. These data, taken together with the restoration of lipid rafts and angiostatin uptake through addition of cholesterol to MCD-treated neutrophils, suggest a role for the lipid rafts in the uptake of angiostatin by activated neutrophils.

It has been established by Tarui et al. that angiostatin interacts with one of its receptors, $\alpha_v\beta_3$ integrin, in a lysine-dependent manner, as shown in β_3-transfected CHO cells (Tarui et al. 2001). Our data also detected integrin β_3 along with flotillin-1 in the co-immunoprecipitated angiostatin complex. Angiostatin co-localized with β_3 integrin, which is one of its known receptors and recycles to and from lipid rafts during chemotaxis (Castel et al. 2001; Fabbri et al. 2005). The finding that blockade of integrin β_3 did not prevent the leading-edge formation in fMLP-activated neutrophils is not

Fig. 9 Effect of angiostatin on TNFα-induced neutrophil migration under flow conditions. Angiostatin inhibits adhesion and transendothelial migration in TNFα-activated cremaster muscle. **a** Rolling flux (cells/min) of leukocytes in post-capillary venules of cremaster muscle at 4, 4.5 and 5 h, along the *x*-axis, after intrascrotal injection of saline ($n=10$), ANG (260 μg/mice) ($n=5$), TNFα (0.05 μg/mice) ($n=9$) and TNFα (0.05 μg/mice)+ANG (260 μg/mice) ($n=5$). *$p<0.05$. Angiostatin is represented as ANG. **b** Rolling velocities (μm/s) of first 20 rolling leukocytes in post-capillary venules of cremaster muscle at 4, 4.5 and 5 h, along the *x*-axis, after intrascrotal injection of saline ($n=10$), ANG (260 μg/mice) ($n=5$), TNFα (0.05 μg/mice) ($n=9$) and TNFα (0.05 μg/mice)+ANG (260 μg/mice) ($n=5$). Angiostatin is represented as ANG. *$p<0.05$. **c** Adhesion (number of cells per 100 μm vessel length) of leukocytes in post-capillary venules of cremaster muscle at 4, 4.5 and 5 h, along the *x*-axis, after intrascrotal injection of saline ($n=10$), ANG (260 μg/mice) ($n=5$), TNFα (0.05 μg/mice) ($n=9$) and TNFα (0.05 μg/mice)+ANG (260 μg/mice) ($n=5$). Angiostatin is represented as ANG. *$p<0.05$. **d** Emigration (number of cells per field of view, i.e., two screens wide) of leukocytes above and below the post-capillary venules of cremaster muscle at 4, 4.5 and 5 h, along the *x*-axis, after intrascrotal injection of saline ($n=10$), ANG (260 μg/mice) ($n=5$), TNFα (0.05 μg/mice) ($n=9$) and TNFα (0.05 μg/mice)+ANG (260 μg/mice) ($n=5$). Angiostatin is represented as ANG. *$p<0.05$. **e** Representative differential interference contrast and H&E stained images of cremaster muscle 5.5 h after intrascrotal injection of saline ($n=10$), ANG (260 μg/mice) ($n=5$), TNFα (0.05 μg/mice) ($n=9$) and TNFα (0.05 μg/mice)+ANG (260 μg/mice) ($n=5$). Angiostatin is represented as ANG. *Thin arrows* indicate adhering leukocytes, whereas the *thick arrows* indicate extravasated leukocytes, which are mainly polymorphonuclear neutrophils in morphology. *Bar* = 50 μm. **f** Angiostatin reduces myeloperoxidase (MPO) in TNFα inflamed cremaster muscle. Myeloperoxidase (MPO) assay of mouse cremaster muscle after intrascrotal injection of saline ($n=10$), ANG (260 μg/mice) ($n=5$), TNFα (0.05 μg/mice) ($n=9$) and TNFα (0.05 μg/mice)+ANG (260 μg/mice) ($n=5$). Angiostatin is represented as ANG. *$p<0.05$

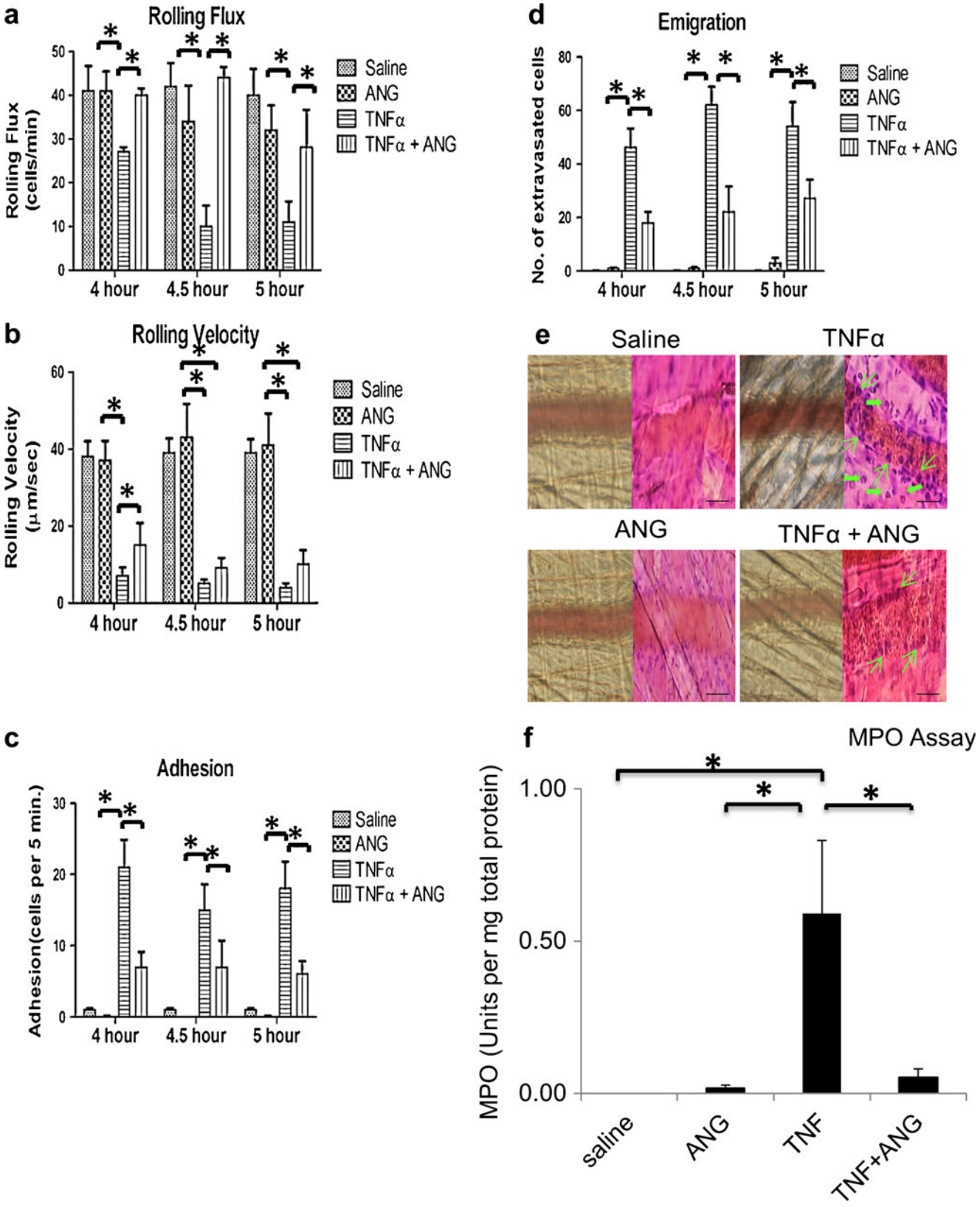

surprising, keeping in mind the well-established role of integrins β_2 and β_1 in neutrophil migration (Harris et al. 2001; Kuijpers et al. 1997; Liu et al. 2012). While the integrin blocking with LM609 antibody did not prevent angiostatin

endocytosis, it restored polarization of neutrophils in the presence of angiostatin and fMLP to suggest that angiostatin and the LM609 antibody bind to the same β_3 integrin. In addition to LM609, another antibody 7E3 is also used to block integrin β_3. Based on the published evidence that 7E3 blocks binding of LM609 to integrin β_3 and that both LM609 and 7E3 are equally effective in blocking angiostatin binding (Puzon-McLaughlin et al. 2000; Artoni et al. 2004; Tarui et al. 2001), we chose to use only LM609. There are three possible explanations for this partial reversal of angiostatin's effects with blockade of β_3 integrin. First, LM609 is an allosteric inhibitor of $\alpha_v\beta_3$ integrin but angiostatin interacts with the RGD binding site on this integrin. Second, it has recently been shown that integrins are dispensable for neutrophil migration (Lammermann et al. 2008). Based upon the lipid raft blocking experiment, we speculate that proteins like flotillin and caveolin-rich microdomains are possibly more important in the process of endocytosis of angiostatin (Castel et al. 2001; Fabbri et al. 2005; Tuluc et al. 2003). Third, angiostatin and LM609 may not be stoichometrically balanced, so that the block was not sufficient. Nevertheless, the data show some interaction of angiostatin with β_3 integrin expressed on neutrophils, resulting in a reversal of the effects of angiostatin. Because LM609 requires cross-linking to activate integrin $\alpha_v\beta_3$ signaling (Tsukada et al. 1995), we believe that LM609 alone would not activate the integrin in neutrophils. While the issue can be fully addressed using integrin $\beta_3^{-/-}$ neutrophils, the fact that LM609 reverses rather than competes with angiostatin suggests that angiostatin might either be acting independently of integrin β_3, or that the LM609-integrin β_3-angiostatin complex might inhibit the angiostatin-mediated downstream small G-protein signaling cascade, as is the case with some chemokine CXCR2 or formyl peptide, fMLP, receptor inverse agonists (Bradley et al. 2009; Mustafa et al. 2012; Wenzel-Seifert et al. 1998). However, more studies are needed to address the interactions of angiostatin with integrin β_3.

Polarization in response to chemo-attractants is a primal event in chemotaxis (Insall 2010). In vitro confocal microscopy on mouse as well as human neutrophils revealed that angiostatin abolished polarization as well as activation of neutrophils in response to fMLP and LPS. The response of angiostatin to non-receptor mediated chemotactic agents such as IL-8 and MIP-2 should also be further explored, as angiostatin inhibits neutrophil chemotaxis in response to IL-8, MIP-2 and Gro-α (Benelli et al. 2002). Hsp-27 induces actin capping and phosphorlyation of hsp-27 is essential for maintaining polarized heads (Jog et al. 2007). Immunoprecipitation data have revealed that hsp-27 binds to both α and β tubulin and inhibits tubulin polymerization (Hino and Hosoya 2003; Hino et al. 2000). While it is still not clear whether inhibition of hsp-27 phosphorylation observed with confocal microscopy and western blots is a direct effect of angiostatin or due to angiostatin-mediated inhibition of MAPKinases observed in our experiments, angiostatin inhibited phosphorylation of hsp-27 and blocked formation of polarized heads. The ability of angiostatin to cause redistribution of and to localize with angiomotin suggests its interactions with angiomotin to inhibit formation of polarized heads in neutrophils. Angiomotin can bind to cdc-42 Rho GTPase activating protein (GAP), Rich1 and produce a hypermigratory state in endothelial and epithelial cells (Gagne et al. 2009; Ernkvist et al. 2008, 2009). Angiostatin can also bind to actin in cultured macrophages and endothelial cells to inhibit their migration and polarization (Dudani et al. 2005; Perri et al. 2007a). Because blockade of β_3 integrin with function blocking antibodies restored polarization in angiostatin-treated neutrophils without altering uptake of angiostatin, it appears that angiostatin may be inducing its actions through its receptors other than β_3 integrin. While some of the molecular mechanisms require further investigation, the in vitro effects of angiostatin on neutrophils are supported by our in vivo intravital microscopic data that angiostatin blocks neutrophil adhesion, emigration and accumulation in cremaster muscles.

We also explored the effects of angiostatin on LPS activated neutrophils. Activated neutrophils perform their roles in innate defense of the host through molecules such as ROS. We found that angiostatin treatment silences generation of ROS in LPS-activated neutrophils. Because F_1F_0 ATP synthase translocates to lipid raft caveolae and also resides in cytosol (Wahl et al. 2005), it is possible that angiostatin and the synthase interact with each other. This possibility is supported through co-immunoprecipitation data showing presence of F_1F_0 ATP synthase in the angiostatin-precipitated immune complex from neutrophils. These results suggest the important role of ATP synthase as a mitochondrial as well as cell surface receptor for angiostatin-mediated inhibition of LPS-induced neutrophil activation. Not only did angiostatin reduce ROS production, we also found that it increased expression of activated caspase-3 and induced apoptosis to silence the neutrophils for good, which is in accordance with earlier observations (Pluskota et al. 2008). Activated neutrophils also generate ROS through p44/42 MAPKinase phosphorylation (Espinosa et al. 2006; Khan et al. 2005; Markvicheva et al. 2010; Zhong et al. 2003), which, in turn, act as signaling molecules (Espinosa et al. 2006; Fialkow et al. 2007). The respiratory burst is also mediated by integrin β_3 signalling (Yan and Novak 1999). Angiostatin significantly inhibited the phosphorylation of p38MAPK and p44/42 MAPK without affecting the levels of total MAPK proteins in LPS-treated neutrophils and these results were validated with pharmacological inhibitors of p38 as well as p44/42 MAPK. Downstream molecules for chemotaxis regulation are in part mediated by phosphorylation of p38 MAPKinase in LPS-treated neutrophils (Jog et al. 2007; Khan et al. 2005; Kutsuna et al. 2004; Lokuta and Huttenlocher 2005; Niggli

2003; Sabroe et al. 2005) and suppression of MAPK signalling by angiostatin may underlie its inhibition of neutrophil migration. LPS-stimulated neutrophils live longer because of suppression of their constitutive apoptosis and they potentially cause more tissue damage through continued production of ROS and ROS also contributes to suppression of apoptosis. Angiostatin not only shut down production of ROS and phosphorylation of p44/42 MAPKinase in activated neutrophils, it also induced robust expression of activated caspase-3, which is central to the induction of apoptosis in neutrophils. We confirmed the role of p38 MAPK in angiostatin-induced caspase-3 expression by showing restoration of caspase-3 cleavage in LPS-treated neutrophils with SB239063 pretreatment, which is a potent inhibitor of p38 MAPK inhibitor.

Collectively, the data show multifaceted effects of angiostatin across a broad spectrum of neutrophil activities. Angiostatin diminishes abilities of activated neutrophils to migrate in vivo and in vitro and silences activated neutrophils through inhibition of signalling and ROS production and silences them for good through induction of apoptosis. Based on the data reported in this manuscript, we propose a schematic model (Fig. 10) to highlight the possible role of

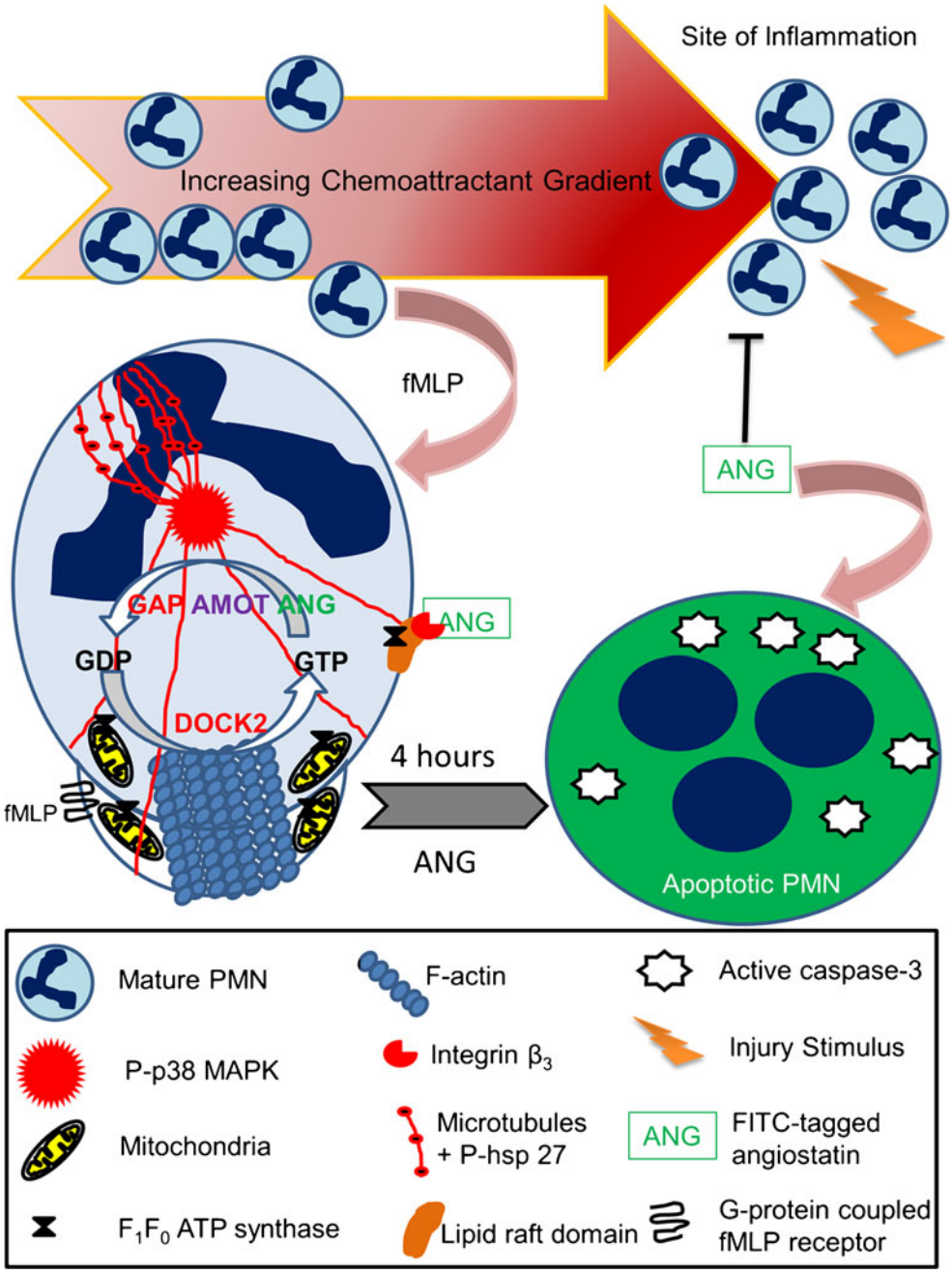

Fig. 10 Schematic diagram for mechanism of action of angiostatin (ANG) in acute inflammation. ANG inhibits neutrophil adhesion as well as trans-endothelial migration in an acute inflammation setting by inhibiting the leading edge actin dynamics. Angiostatin is endocytozed in activated neutrophils via lipid raft domains, which express integrin $\alpha_v\beta_3$ as well as F_1F_0 ATP synthase. We hypothesize that ANG binds to a GTPase activating protein (GAP) associated angiomotin (AMOT) that inhibits guanosine triphophate (GTP) recycling required for F-actin aggregation at the leading edge, thereby inhibiting neutrophil chemotaxis. Shut-down of the mitochondrial ATP synthesis upon inhibition of F_1F_0 ATP synthase leads to mitochondrial redox inhibition and reduction in ROS production and ultimately induces apoptosis, as evidenced through the presence of apoptotic nuclear bodies (depicted in *blue*) after LPS and 4 h angiostatin incubation. For further explanation, refer to text

angiostatin in acute inflammation. While further work is needed to establish a precise relationship between the various angiostatin-binding proteins as receptors and (or) downstream signaling molecules, the data create the possibility of devising anti-inflammatory therapies based on angiostatin.

Conclusions

Taken together, the data show abilities of angiostatin to complex with flotillin-1, integrin $\alpha_v\beta_3$, as well as F_1F_0 ATP synthase and attenuate polarization, MAPK phosphorylation, mitochondrial activation and ROS production while activating caspase-3 expression and inducing apoptosis in activated neutrophils. The in vitro effects of angiostatin translate into in vivo inhibition of migration of neutrophils in post-capillary venules in TNFα-treated cremaster muscle. These data are of significance because of the critical double-edged role of neutrophils in numerous acute inflammatory pathologies such as sepsis, transfusion-induced injuries and acute pancreatitis that require modulation of activated neutrophils to preserve their beneficial effects and minimize deleterious tissue effects.

Acknowledgments We would like to thank Dr. Wolfgang Kuebler for providing valuable comments on the manuscript and Mr. Daryoush Hajinezhad for technical assistance with the confocal microscope. The study was funded through a grant from the Natural Sciences and Engineering Research Council of Canada to Dr. Baljit Singh. Dr. Aulakh was supported through a Dean's Scholarship from the College of Graduate Studies and Research, University of Saskatchewan.

Authorship G.K.A., L.L. and B.S. planned the experiments, analyzed data and wrote the manuscript. G.K.A. carried out all the experiments. Y.B. helped in angiostatin post-treatment confocal experiments on human neutrophils.

References

Allen L-AH (2007) Immunofluorescence and confocal microscopy of neutrophils. Methods Mol Biol 412:273–287

Amulic B, Cazalet C, Hayes GL, Metzler KD, Zychlinsky A (2012) Neutrophil function: from mechanisms to disease. Annu Rev Immunol 30:459–489

Aoshiba K, Yasui S, Hayashi M, Tamaoki J, Nagai A (1999) Role of p38-mitogen-activated protein kinase in spontaneous apoptosis of human neutrophils. J Immunol 162:1692–1700

Artoni A, Li J, Mitchell B, Ruan J, Takagi J, Springer TA, French DL, Coller BS (2004) Integrin beta 3 regions controlling binding of murine mAb 7E3: implications for the mechanism of integrin alphaIIbbeta3 activation. Proc Natl Acad Sci U S A 101:13114–13120

Barreiro O, De La Fuente H, Mittelbrunn M, Sánchez-Madrid F (2007) Functional insights on the polarized redistribution of leukocyte integrins and their ligands during leukocyte migration and immune interactions. Immunol Rev 218:147–164

Barreiro O, Martín P, González-Amaro R, Sánchez-Madrid F (2010) Molecular cues guiding inflammatory responses. Cardiovasc Res 86:174–182

Benelli R, Morini M, Carrozzino F, Ferrari N, Minghelli S, Santi L, Cassatella M, Noonan DM, Albini A (2002) Neutrophils as a key cellular target for angiostatin: implications for regulation of angiogenesis and inflammation. FASEB J 16:267–269

Bradley ME, Bond ME, Manini J, Brown Z, Charlton SJ (2009) SB265610 is an allosteric, inverse agonist at the human CXCR2 receptor. Br J Pharmacol 158:328–338

Castel S, Pagan R, Mitjans F, Piulats J, Goodman S, Jonczyk A, Huber F, Vilaro S, Reina M (2001) RGD peptides and monoclonal antibodies, antagonists of alpha(v)-integrin, enter the cells by independent endocytic pathways. Lab Invest 81:1615–1626

Chavakis T, Athanasopoulos A, Rhee JS, Orlova V, Schmidt-Woll T, Bierhaus A, May AE, Celik I, Nawroth PP, Preissner KT (2005) Angiostatin is a novel anti-inflammatory factor by inhibiting leukocyte recruitment. Blood 105:1036–1043

Dudani AK, Ben-Tchavtchavadze M, Porter S, Tackaberry E (2005) Angiostatin and plasminogen share binding to endothelial cell surface actin. Biochem Cell Biol 83:28–35

Dudani AK, Mehic J, Martyres A (2007) Plasminogen and angiostatin interact with heat shock proteins. Mol Cell Biochem 300:197–205

Eddy RJ, Pierini LM, Maxfield FR (2002) Microtubule asymmetry during neutrophil polarization and migration. Mol Biol Cell 13:4470–4483

Ernkvist M, Birot O, Sinha I, Veitonmaki N, Nystrom S, Aase K, Holmgren L (2008) Differential roles of p80- and p130- angiomotin in the switch between migration and stabilization of endothelial cells. Biochim Biophys Acta, Mol Cell Res 1783:429–437

Ernkvist M, Persson NL, Audebert S, Lecine P, Sinha I, Liu M, Schlueter M, Horowitz A, Aase K, Weide T, Borg JP, Majumdar A, Holmgren L (2009) The Amot/Patj/Syx signaling complex spatially controls RhoA GTPase activity in migrating endothelial cells. Blood 113:244–253

Espinosa A, Leiva A, Peña M, Müller M, Debandi A, Hidalgo C, Angélica Carrasco M, Jaimovich E (2006) Myotube depolarization generates reactive oxygen species through NAD(P)H oxidase; ROS-elicited Ca2+ stimulates ERK, CREB, early genes. J Cell Phys 209:379–388

Fabbri M, Di Meglio S, Gagliani MC, Consonni E, Molteni R, Bender JR, Tacchetti C, Pardi R (2005) Dynamic partitioning into lipid rafts controls the endo-exocytic cycle of the alphaL/beta2 integrin, LFA-1, during leukocyte chemotaxis. Mol Biol Cell 16:5793–5803

Fialkow L, Wang Y, Downey GP (2007) Reactive oxygen and nitrogen species as signaling molecules regulating neutrophil function. Free Radic Biol Med 42:153–164

Gagne V, Moreau J, Plourde M, Lapointe M, Lord M, Gagnon E, Fernandes MJ (2009) Human angiomotin-like 1 associates with an angiomotin protein complex through its coiled-coil domain and induces the remodeling of the actin cytoskeleton. Cell Motil Cytoskeleton 66:754–768

Hamacher J, Lucas R, Lijnen HR, Buschke S, Dunant Y, Wendel A, Grau GE, Suter PM, Ricou B (2002) Tumor necrosis factor-{alpha} and angiostatin are mediators of endothelial cytotoxicity in bronchoalveolar lavages of patients with acute respiratory distress syndrome. Am J Respir Crit Care Med 166:651

Harris ES, Shigeoka AO, Li W, Adams RH, Prescott SM, McIntyre TM, Zimmerman GA, Lorant DE (2001) A novel syndrome of variant leukocyte adhesion deficiency involving defects in adhesion mediated by beta1 and beta2 integrins. Blood 97:767–776

Hendey B, Lawson M, Marcantonio EE, Maxfield FR (1996) Intracellular calcium and calcineurin regulate neutrophil motility on vitronectin through a receptor identified by antibodies to integrins αv and β3. Blood 87:2038–2048

Hermel M, Dailey W, Hartzer MK (2010) Efficacy of plasmin, microplasmin, and streptokinase-plasmin complex for the in vitro degradation of fibronectin and laminin- implications for vitreoretinal surgery. Curr Eye Res 35:419–424

Hino M, Hosoya H (2003) Small heat shock protein Hsp27 directly binds to alpha/beta tubulin heterodimer and inhibits DMSO-induced tubulin polymerization. Biomed Res 24:27–30

Hino M, Kurogi K, Okubo MA, Murata-Hori M, Hosoya H (2000) Small heat shock protein 27 (HSP27) associates with tubulin/microtubules in HeLa cells. Biochem Biophys Res Commun 271:164–169

Insall RH (2010) Understanding eukaryotic chemotaxis: a pseudopod-centred view. Nat Rev Mol Cell Biol 11:453–458

Insall RH, Machesky LM (2009) Actin dynamics at the leading edge: from simple machinery to complex networks. Dev Cell 17:310–322

Jog NR, Jala VR, Ward RA, Rane MJ, Haribabu B, McLeish KR (2007) Heat shock protein 27 regulates neutrophil chemotaxis and exocytosis through two independent mechanisms. J Immunol 178:2421–2428

Jurasz P, Santos-Martinez MJ, Radomska A, Radomski MW (2006) Generation of platelet angiostatin mediated by urokinase plasminogen activator: effects on angiogenesis. J Thromb Haemost 4:1095–1106

Kenan DJ, Wahl ML (2005) Ectopic localization of mitochondrial ATP synthase: a target for anti-angiogenesis intervention? J Bioenerg Biomembr 37:461

Khan AI, Heit B, Andonegui G, Colarusso P, Kubes P (2005) Lipopolysaccharide: a p38 MAPK-dependent disrupter of neutrophil chemotaxis. Microcirc 12:421–432

Kuijpers TW, Van Lier RA, Hamann D, de Boer M, Thung LY, Weening RS, Verhoeven AJ, Roos D (1997) Leukocyte adhesion deficiency type 1 (LAD-1)/variant. A novel immunodeficiency syndrome characterized by dysfunctional beta2 integrins. J Clin Invest 100:1725–1733

Kutsuna H, Suzuki K, Kamata N, Kato T, Hato F, Mizuno K, Kobayashi H, Ishii M, Kitagawa S (2004) Actin reorganization and morphological changes in human neutrophils stimulated by TNF, GM-SCF and G-CSF: The role of MAP kinases. Am J Physiol Cell Physiol 286:C55–C64

Lammermann T, Bader BL, Monkley SJ, Worbs T, Wedlich-Soldner R, Hirsch K, Keller M, Forster R, Critchley DR, Fassler R, Sixt M (2008) Rapid leukocyte migration by integrin-independent flowing and squeezing. Nature 453:51–55

Lawson MA, Maxfield FR (1995) Ca2+− and calcineurin-dependent recycling of an integrin to the front of migrating neutrophils. Nature 377:75–79

Lee TY, Muschal S, Pravda EA, Folkman J, Abdollahi A, Javaherian K (2009) Angiostatin regulates the expression of antiangiogenic and proapoptotic pathways via targeted inhibition of mitochondrial proteins. Blood 114:1987–1998

Ley K, Laudanna C, Cybulsky MI, Nourshargh S (2007) Getting to the site of inflammation: the leukocyte adhesion cascade updated. Nat Rev Immunol 7:678–689

Liu L, Kubes P (2003) Molecular mechanisms of leukocyte recruitment: organ-specific mechanisms of action. Thromb Haemost 89:213–220

Liu L, Aerbajinai W, Ahmed SM, Rodgers GP, Angers S, Parent CA (2012) Radil controls neutrophil adhesion and motility through beta2-integrin activation. Mol Biol Cell 23:4751–4765

Lokuta MA, Huttenlocher A (2005) TNF-α promotes a stop signal that inhibits neutrophil polarization and migration via a p38 MAPK pathway. J Leukoc Biol 78:210–219

Lucas R, Lijnen HR, Suffredini AF, Pepper MS, Steinberg KP, Martin TR, Pugin J (2002) Increased angiostatin levels in bronchoalveolar lavage fluids from ARDS patients and from human volunteers after lung instillation of endotoxin. Thromb Haemost 87:966–971

Markvicheva KN, Gorokhovatskii AY, Mishina NM, Mudrik NN, Vinokurov LM, Luk'Yanov SA, Belousov VV (2010) Signaling function of phagocytic NADPH oxidase: activation of MAP kinase cascades in phagocytosis. Russ J Bioorg Chem 36:124–129

Moon C, Han JR, Park HJ, Hah JS, Kang JL (2009) Synthetic RGDS peptide attenuates lipopolysaccharide-induced pulmonary inflammation by inhibiting integrin signaled MAP kinase pathways. Respir Res 10:18

Mustafa S, See HB, Seeber RM, Armstrong SP, White CW, Ventura S, Ayoub MA, Pfleger KD (2012) Identification and profiling of novel alpha1A-adrenoceptor-CXC chemokine receptor 2 heteromer. J Biol Chem 287:12952–12965

Niggli V (2003) Signaling to migration in neutrophils: importance of localized pathways. Int J Biochem Cell Biol 35:1619–1638

Nuzzi PA, Lokuta MA, Huttenlocher A (2007) Analysis of neutrophil chemotaxis. Methods Mol Biol 370:23–36

O'Mahony CA, Seidel A, Albo D, Chang H, Tuszynski GP, Berger DH (1998) Angiostatin generation by human pancreatic cancer. J Surg Res 77:55–58

Perri SR, Annabi B, Galipeau J (2007a) Angiostatin inhibits monocyte/macrophage migration via disruption of actin cytoskeleton. FASEB J 21:3928

Perri SR, Martineau D, Francois M, Lejeune L, Bisson L, Durocher Y, Galipeau J (2007b) Plasminogen Kringle 5 blocks tumor progression by antiangiogenic and proinflammatory pathways. Mol Cancer Therap 6:441–449

Pluskota E, Soloviev DA, Szpak D, Weber C, Plow EF (2008) Neutrophil apoptosis: selective regulation by integrin αMβ2 ligands. J Immunol 181:3609–3619

Puzon-McLaughlin W, Kamata T, Takada Y (2000) Mutliple discontinuous ligand-mimetic antibody binding sites define a ligand-binding pocket in integrin alpha(IIb)beta3. J Biol Chem 275:7795–7802

Rainger GE, Buckley CD, Simmons DL, Nash GB (1999) Neutrophils sense flow-generated stress and direct their migration through αVβ3-integrin. Am J Physiol Heart Circ Physiol 276:H858–H864

Sabroe I, Dower SK, Whyte MK (2005) The role of Toll-like receptors in the regulation of neutrophil migration, activation and apoptosis. Clin Infect Dis 41:S421–S426

Scapini P, Nesi L, Morini M, Tanghetti E, Belleri M, Noonan D, Presta M, Albini A, Cassatella MA (2002) Generation of biologically active angiostatin kringle 1–3 by activated human neutrophils 1. J Immunol 168:5798–5804

Schierwagen C, Bylund-Fellenius AC, Lundberg C (1990) Improved method for quantification of tissue PMN accumulation measured by myeloperoxidase activity. J Pharm Meth 23:179–186

Sharma MR, Rothman V, Tuszynski GP, Sharma MC (2006) Antibody-directed targeting of angiostatin's receptor annexin II inhibits Lewis Lung Carcinoma tumor growth via blocking of plasminogen activation: possible biochemical mechanism of angiostatin's action. Exp Mol Pathol 81:136–145

Singh B, Fu C, Bhattacharya J (2000) Vascular expression of the αvβ3-integrin in lung and other organs. Am J Physiol Lung Cell Mol Physiol 278:217–226

Singh B, Janardhan KS, Kanthan R (2005) Expression of angiostatin, integrin αvβ3, and vitronectin in human lungs in sepsis. Exp Lung Res 31:771–782

Singh RD, Marks DL, Holicky EL, Wheatley CL, Kaptzan T, Sato SB, Kobayashi T, Ling K, Pagano RE (2010) Gangliosides and β1-integrin are required for caveolae and membrane domains. Traffic 11:348–360

Spisani S, Falzarano S, Traniello S, Nalli M, Selvatici R (2005) A 'pure' chemoattractant formylpeptide analogue triggers a specific signalling pathway in human neutrophil chemotaxis. FEBS J 272:883–891

Syed SP, Martin AM, Haupt HM, Arenas-Elliot CP, Brooks JJ (2007) Angiostatin receptor annexin II in vascular tumors including angiosarcoma. Hum Pathol 38:508–513

Tabruyn SP, Griffioen AW (2007) Molecular pathways of angiogenesis inhibition. Biochem Biophys Res Commun 355:1–5

Tarui T, Miles LA, Takada Y (2001) Specific interaction of angiostatin with integrin alpha(v)beta(3) in endothelial cells. J Biol Chem 276: 39562–39568

Troyanovsky B, Levchenko T, Mansson G, Matvijenko O, Holmgren L (2001) Angiomotin an angiostatin binding protein that regulates

endothelial cell migration and tube formation. J Cell Biol 152:1247–1254

Tsukada H, Ying X, Fu C, Ishikawa S, McKeown-Longo P, Albelda S, Bhattacharya S, Bray BA, Bhattacharya J (1995) Ligation of endothelial alpha v beta 3 integrin increases capillary hydraulic conductivity of rat lung. Circ Res 77:651–659

Tuluc F, Meshki J, Kunapuli SP (2003) Membrane lipid microdomains differentially regulate intracellular signaling events in human neutrophils. Int Immunopharmacol 3:1775–1790

Underwood DC, Osborn RR, Bochnowicz S, Webb EF, Rieman DJ, Lee JC, Romanic AM, Adams JL, Hay DWP, Griswold DE (2000) SB 239063, a p38 MAPK inhibitor, reduces neutrophilia, inflammatory cytokines, MMP-9, and fibrosis in lung. Am J Physiol Lung Cell Mol Physiol 279:L895–L902

Wahl ML, Kenan DJ, Gonzalez-Gronow M, Pizzo SV (2005) Angiostatin's molecular mechanism: aspects of specificity and regulation elucidated. J Cell Biochem 96:242–261

Warejcka DJ, Twining SS (2005) Specific conformational changes of plasminogen induced by chloride ions, 6-aminohexanoic acid and benzamidine, but not the overall openness of plasminogen regulate, production of biologically active angiostatins. Biochem J 392:703–712

Wells CD, Fawcett JP, Traweger A, Yamanaka Y, Goudreault M, Elder K, Kulkarni S, Gish G, Virag C, Lim C (2006) A Rich1/Amot complex regulates the Cdc42 GTPase and apical-polarity proteins in epithelial cells. Cell 125:535–548

Wenzel-Seifert K, Hurt CM, Seifert R (1998) High constitutive activity of the human formyl peptide receptor. J Biol Chem 273:24181–24189

Westphal JR, Van't Hullenaar R, Geurts-Moespot A, Sweep FCJG, Verheijen JH, Bussemakers MMG, Askaa J, Clemmensen I, Eggermont AAM, Ruiter DJ, De Waal RMW (2000) Angiostatin generation by human tumor cell lines: Involvement of plasminogen activators. Int J Cancer 86:760–767

Witko-Sarsat V (2010) Apoptosis, cell death and inflammation. J Innate Immunity 2:201–203

Witko-Sarsat V, Rieu P, Descamps-Latscha B, Lesavre P, Halbwachs-Mecarelli L (2000) Neutrophils: molecules, functions and pathophysiological aspects. Lab Invest 80:617–654

Wong CHY, Heit B, Kubes P (2010) Molecular regulators of leucocyte chemotaxis during inflammation. Cardiovasc Res 86:183–191

Yan SR, Novak MJ (1999) Diverse effects of neutrophil integrin occupation on respiratory burst activation. Cell Immunol 195:119–126

Yoo SK, Lam PY, Eichelberg MR, Zasadil L, Bement WM, Huttenlocher A (2012) The role of microtubules in neutrophil polarity and migration in live zebrafish. J Cell Sci 125:5702–5710

Zhong B, Jiang K, Gilvary DL, Epling-Burnette EK, Ritchey C, Liu J, Jackson RJ, Hong-Geller E, Wei S (2003) Human neutrophils utilize a Rac/Cdc42-dependent MAPK pathway to direct intracellular granule mobilization toward ingested microbial pathogens. Blood 101: 3240–3248